Searching for exclusive leptoquarks with the Nambu-Jona-Lasinio composite model at the LHC and HL-LHC

S. Ajmal [a,b] **J.T. Gaglione** [c] **A. Gurrola** [c] **O. Panella** [b] **M. Presilla** [d]
F. Romeo [c] **H. Sun** [e] **and S.-S. Xue** [f,g,b,h]

[a]*Dipartimento di Fisica e Geologia, Univeristà degli Studi di Perugia,*
Via A. Pascoli, I-06123 Perugia, Italy

[b]*Istituto Nazionale di Fisica Nucleare (INFN), Sezione di Perugia,*
Via A. Pascoli, I-06123, Perugia, Italy

[c]*Department of Physics and Astronomy, Vanderbilt University,*
Nashville, TN, 37235, U.S.A.

[d]*Institute for Experimental Particle Physics (ETP), Karlsruhe Institute of Technology (KIT),*
Wolfgang-Gaede-Straße 1, 76131 Karlsruhe, Germany

[e]*Institute of Theoretical Physics, School of Physics, Dalian University of Technology,*
No. 2 Linggong Road, Dalian, Liaoning, 116024, P. R. China

[f]*ICRANet,*
Piazzale della Repubblica, 10-65122, Pescara, Italy

[g]*Physics Department, Sapienza University of Rome,*
Piazzale Aldo Moro 5, 00185 Roma, Italy

[h]*ICTP-AP, University of Chinese Academy of Sciences,*
Beijing, China

E-mail: sehar.ajmal@cern.ch, jethrogaglione@gmail.com,
alfredo.gurrola@vanderbilt.edu, orlando.panella@pg.infn.it,
matteo.presilla@cern.ch, francesco.romeo@cern.ch, haosun@dlut.edu.cn,
she-sheng.xue@cern.ch

ABSTRACT: We present a detailed study concerning a new physics scenario involving four fermion operators of the Nambu-Jona-Lasinio type characterized by a strong-coupling ultraviolet fixed point where composite particles are formed as bound states of elementary fermions at the scale $\Lambda = \mathcal{O}(\text{TeV})$. After implementing the model in the Universal FeynRules Output format, we focus on the phenomenology of the scalar leptoquarks at the LHC and the High-Luminosity option. Leptoquark particles have undergone extensive scrutiny in the literature and experimental searches, primarily relying on pair production and, more recently, incorporating single, Drell-Yan t-channel, and lepton-induced processes. This study marks, for the first time, the examination of these production modes at varying jet multiplicities. Novel mechanisms emerge, enhancing the total production cross section. A global strategy is devised

to capture all final state particles produced in association with leptoquarks or originating from their decay, which we termed "exclusive", in an analogy to the nomenclature used in nuclear reactions. The assessment of the significance in current and future LHC runs, focusing on the case of a leptoquark coupling to a muon–c quark pair, reveals greater sensitivity compared to ongoing searches. Given this heightened discovery potential, we advocate the incorporation of exclusive leptoquark searches in future investigations at the LHC.

Contents

1   Introduction

Thanks to its remarkably strong quantitative agreement with experimental results over the past decades, the Standard Model (SM) has been solidified as a cornerstone of elementary particle physics. Nonetheless, it is regarded as an effective theory that falls short in encompassing several foundational aspects of both theoretical and observed particle physics. Numerous extensions have been put forward, suggesting specific tests to challenge the SM at the LHC. Regrettably, all of these searches have thus far yielded a negative outcome in the quest for detecting new physics and have placed significant constraints on many beyond-the-SM (BSM) models in mass scales up to a few TeV [1–8].

Therefore, the question arises as to whether ongoing searches have exhaustively explored all avenues, or if unprecedented aspects can yet be harnessed to devise better methods that would probe yet uncharted territory. In this paper, we present an in-depth phenomenological study of a novel composite scenario based on Nambu-Jona-Lasinio (NJL) type four-fermion operators recently proposed in [9–11]. The model is characterized by a strong coupling ultraviolet (UV) fixed point where composite particles arise as bound states of SM elementary fermions. The counterpart of a strong-coupled electron system is studied [12] in condensed-matter physics. The effective four-fermion interactions considered in this new model are motivated by theoretical inconsistencies [13–15] between the SM bilinear Lagrangian of chiral gauged fermions and the UV regularization of some unknown dynamics, such as quantum gravity. These inconsistencies imply, at high energies, quadrilinear effective operators (four-fermion interactions) of the NJL or Einstein-Cartan type [16–18]. A first phenomenological study related to the production at the LHC of composite fermions in the gauge symmetric phase of this NJL model was conducted in [19] where a recent CMS analysis [20] of the dilepton plus dijet final state was recast to derive constraints on the parameter space of the NJL model. More recent studies of the XENON1T experiment [21], neutrino-less double

beta decay [22], and W-boson mass tension [23] addressed the broken-gauge phase of the model. In this work we specifically address the phenomenology at the LHC of the scalar leptoquarks (LQs) arising in the gauge symmetric phase of the model, thus delving into one of the most extensively studied subjects in the BSM landscape. While reviewing current investigations, production modes, and search strategies, we investigate the potential for new mechanisms and approaches at the LHC.

LQs are hypothetical particles that carry both lepton number L and baryon number B, have a fractional electric charge, and can be either scalar (spin 0) or vector (spin 1) particles. They offer a natural explanation for the symmetry between the quark and lepton families, attempting to pave the way toward matter unification. They inherently appear in many well-motivated extensions of the SM that endeavor to unify the fundamental interactions, such as grand unified theories [24–29], technicolor models [30–33], and compositeness scenarios [34, 35], as well as R-parity violating supersymmetry [36–45], and as mediators of dark matter-SM interactions [46]. More recently, LQs have gained enhanced interest, as they provide a suitable explanation for a series of anomalies observed in several precision measurements: the $B \to D^*$ anomaly reported by BaBar [47, 48], Belle [49], and LHCb [50] that could be explained by the mediation of an intermediate LQ scalar [51–63]; the muon anomalous magnetic moment $(g-2)_\mu$ measurement from the E989 and E821 collaborations [64, 65] which could be resolved assuming the existence of LQs [64–81]; the charged proton radius obtained from muon Lamb shift [82], and atomic parity violation [83, 84], where low-energy corrections via virtual LQ scalars and internal loop diagrams can contribute. In a search for a LQ coupling to a τ lepton and a b quark, the CMS collaboration has reported an excess with a significance of 2.8 standard deviations above the SM expectation using Run 2 data [85], though consistency with the SM prediction is observed in a similar search from the ATLAS collaboration [86].

Both the ATLAS and the CMS collaborations have a broad LQ search program that covers various particle hypotheses and different lepton-quark-LQ vertex couplings λ. The main production modes considered are illustrated in figure 1 (a–d) and have been extensively discussed in literature [87–104]. The majority of the analyses rely on the LQ pair production mode in figure 1 (c) [2, 105–138], which does not depend on λ. Some searches are designed to intercept the single LQ production process in figure 1 (b) [86, 139–141] or the single and pair productions together [7, 86, 142], as the former brings enhanced sensitivity due to a cross section that varies as a function of λ^2. A recent investigation [143] added further Drell-Yan dilepton t-channel contributions as displayed in figure 1 (a) and [144] was designed specifically for this process, whose cross section depends on λ^4. An additional recent search relies on lepton-induced processes [145], as that in figure 1 (d).

Upon reviewing the existing literature and LHC searches, a noteworthy observation emerges: the generation of LQs via t-channel, single, and pair production processes is solely regarded in terms of their primary production modes. No studies have been carried out to explore the implications of these production mechanisms at various jet multiplicities, assuming that a jet is originating from either a gluon or a quark. Nevertheless, previous research [146–153] has demonstrated that such an approach could amplify the discovery potential by incorporating additional signal sources while effectively reducing the SM background. In this work, we pursue this effort and investigate how LQs would manifest in association with
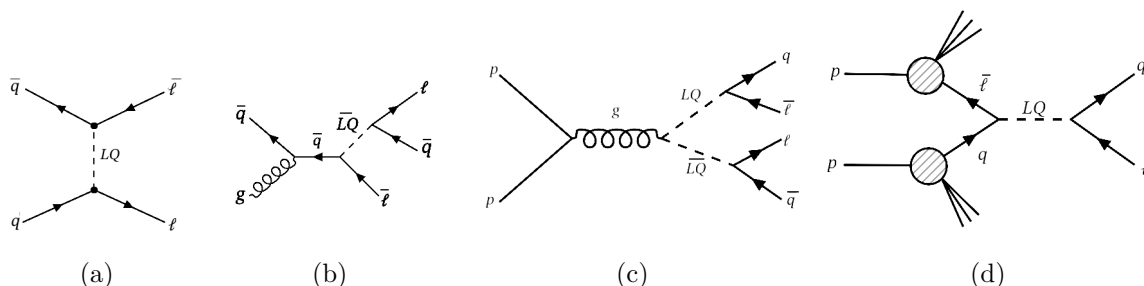
Figure 1. Examples of Feynman diagrams for the Drell-Yan t-chnnel (a), single (b), pair (c), and lepton-induced (d) production modes considered at the LHC.

jets. Our investigation uncovers new production mechanisms and topological aspects not yet considered in ongoing searches. Furthermore, we devise a comprehensive strategy to look for LQs, taking into account all signal contributions. For the case of the lepton-induced process, we undertake a study to separate elastic and inelastic contributions. Our findings reveal that the sensitivity achieved surpasses that of all ongoing searches. This new approach developed here for the specific case of LQs can be adapted and applied in searches for any type of particle to enhance further the expected sensitivity.

In section 2, we introduce the reference LQ model utilized in this analysis, while in section 3 we delve into its implementation and the generation of the signal samples. Section 4 describes the LQ production modes in conjunction with jets and touches upon the possibility of distinguishing elastic and inelastic lepton-induced processes. In section 5 and section 6, we present a global strategy for the detection of LQs based on our findings, as well as the anticipated sensitivity results at both the LHC and the High-Luminosity (HL)-LHC. Finally, in section 7, we summarize the work with some closing remarks.

2   Nambu-Jona-Lasinio composite leptoquark model

The No-Go theorem [13–15] shows that, as a renormalizable quantum field theory at infrared (IR) low energies, the SM *bilinear* fermion Lagrangian at UV cutoff Λ_{cut} suffers theoretical inconsistencies with SM chiral gauge symmetries and fermion spectra at low energies. This implies that new physics at the UV scale Λ_{cut} effectively presents *quadrilinear* operators $G_{\text{cut}}\bar{\psi}_L^f\psi_R^f\bar{\psi}_R^f\psi_L^f$ ($G_{\text{cut}} \propto \Lambda_{\text{cut}}^{-2}$) [9, 10] of NJL or Einstein-Cartan type. They are SM gauge symmetric interactions of SM left- and right-handed fermions (ψ_L^f, ψ_R^f) in the family "f". The strong coupling $g_{\text{cut}} = G_{\text{cut}}\Lambda_{\text{cut}}^2 > 1$ dynamics leads to massive composite bosons $\Pi^f \sim (\bar{\psi}_R^f\psi_L^f)$ and fermions $F_R^f \sim \psi_R^f(\bar{\psi}_R^f\psi_L^f) \sim \psi_R^f\Pi^f$ [154–156]. They carry SM charges and couple to massless SM gauge bosons in a gauge-invariant manner. The effective SM gauge symmetric and renormalizable theory realizes in the scaling domain of the UV fixed point g_{cut}^* at the composite scale $\Lambda \ll \Lambda_{\text{cut}}$ [10, 157]. As the energy scale decreases below Λ, the effective theory undergoes [11] a phase transition of composite particles decays into their constituents and spontaneous SM symmetries breaking via the top-quark channel $(\bar{t}_L t_R \bar{t}_R t_L)$, leading to the SM at the electroweak scale $v \approx 246\,\text{GeV}$ [158]. The scale $\Lambda = \mathcal{O}(\text{TeV})$ is estimated by using the top quark and Higgs boson masses and extrapolating the renormalization-group solution to the high-energy regime [159].

Bosons Π_a^Q	Charge $Q_i = Y + t_{3L}^i$,	$SU_L(2)$ 3-isospin t_{3L}^i,	$U_Y(1)$ charge Y,	$SU_c(3)$ color a,	LQ
$\Pi_a^{+5/3} \propto \bar{e}_R u_{La}$	$+5/3$	$+1/2$	$+7/6$	3	$R_2^{+5/3}$
$\Pi_a^{-1/3} \propto \bar{\nu}_R^e d_{La}$	$-1/3$	$-1/2$	$+1/6$	3	$\tilde{R}_2^{-1/3}$
$\Pi_{u_a}^{+2/3} \propto \bar{\nu}_R^e u_{La}$	$+2/3$	$+1/2$	$+1/6$	3	$\tilde{R}_2^{+2/3}$
$\Pi_{d_a}^{+2/3} \propto \bar{e}_R d_{La}$	$+2/3$	$-1/2$	$+7/6$	3	$R_2^{+2/3}$
$\Pi_a^{-5/3} \propto \bar{u}_{Ra} e_L$	$-5/3$	$-1/2$	$-7/6$	3	$R_2^{-5/3}$
$\Pi_a^{+1/3} \propto \bar{d}_{Ra} \nu_L^e$	$+1/3$	$+1/2$	$-1/6$	3	$\tilde{R}_2^{+1/3}$
$\Pi_{u_a}^{-2/3} \propto \bar{u}_{Ra} \nu_L^e$	$-2/3$	$+1/2$	$-7/6$	3	$R_2^{-2/3}$
$\Pi_{d_a}^{-2/3} \propto \bar{d}_{Ra} e_L$	$-2/3$	$-1/2$	$-1/6$	3	$\tilde{R}_2^{-2/3}$

Table 1. Composite bosons, their constituents, standard model charges, and corresponding leptoquark according to the nomenclature used in [160, 161] for the first generation of standard model fermions.

Composite bosons Π^f and fermions F^f spectra at the Λ scale offer a vast range of new searches and tests of the SM, as shown in [19]. In this article, we study the phenomenological analysis of composite boson states $\Phi \sim (\bar{\ell}_R q_L)$ with fractional electric charge, or LQ, as listed in table 1. Their SM gauge charges are the sum of the SM gauge charges of their fermionic constituents. The gauge-invariant kinetic Lagrangian is

$$(D_\mu \Phi)^\dagger (D_\mu \Phi) + M_\Pi^2 \Phi^\dagger \Phi, \tag{2.1}$$

with covariant derivative,

$$D_\mu = \partial_\mu + ig_1 Y B_\mu + \frac{1}{2} ig_2 \sigma_i W^i{}_\mu + ig_3 T^a G^a{}_\mu \tag{2.2}$$

where Y is the LQ hypercharge, σ_i are the standard Pauli matrices and T^a are the Gell-Mann matrices. Moreover, g_1, g_2, and g_3 are the SM gauge couplings for the respective groups. In eq. (2.1) $SU_c(3)$ triplet LQ bosons form $SU_L(2)$ doublets. Identification of doublets in terms of hypercharge is given as $\Pi_{1/6}^a = \begin{pmatrix} \Pi_{u_a}^{2/3} \\ \Pi_a^{-1/3} \end{pmatrix}$ and $\Pi_{7/6}^a = \begin{pmatrix} \Pi_a^{5/3} \\ \Pi_{d_a}^{2/3} \end{pmatrix}$. The effective coupling between a LQ composite boson and its two constituents can be written as effective contact interactions,

$$\begin{aligned} \mathcal{L}_{CI} = &\, g_{\Pi_{5/3}} (\bar{e}_R u_{La}) \Pi_a^{-5/3} + g_{\Pi_{1/3}} (\bar{\nu}_R^e d_{La}) \Pi_a^{1/3} + g_{\Pi_{-2/3}} (\bar{\nu}_R^e u_{La}) \Pi_{u_a}^{-2/3} \\ &+ g_{\Pi_{-2/3}} (\bar{e}_R d_{La}) \Pi_{d_a}^{-2/3} + \text{h.c.} \end{aligned} \tag{2.3}$$

where the LQ effective Yukawa coupling $g_{\Pi_i} = (F_{\Pi_i}/\Lambda)^2 \sim \mathcal{O}(1)$. The g_{Π_i} parameter defines the decay width (as calculated in [19] for composite bosons with integer charge) via the formula $\Gamma(q\ell) = (g_{\Pi_i}^2 m_\Pi)/16\pi$ that coincides with the general formula used for a scalar LQ (see [160]). For the sake of simplicity and to align to the notation commonly used in experiments (see e.g. [7, 85]) we will use λ to stand for g_{Π_i} in the sections below. The effective interacting Lagrangian (2.1)–(2.3) at the scale Λ is dimension-4 renormalizable, namely independent from the cutoff Λ_{cut}. We tabulate the four quark-lepton composite bosons $\Pi_a^{5/3}$, $\Pi_a^{-1/3}$, $\Pi_{u_a}^{2/3}$ and $\Pi_{d_a}^{2/3}$, identified by constituent fermions and SM gauge charges.

Their conjugated fields are $(\Pi_a^{5/3})^\dagger = \Pi_a^{-5/3}$, $(\Pi_a^{-1/3})^\dagger = \Pi_a^{1/3}$ and $(\Pi_{u_a}^{2/3})^\dagger = \Pi_{d_a}^{-2/3}$, and $(\Pi_{d_a}^{2/3})^\dagger = \Pi_{u_a}^{-2/3}$. The renormalized LQ bosons $\Pi_a^Q = Z_\Pi^{-1/2} \bar{\ell}_R q_{La}$ with the form-factor $Z_\Pi^{-1/2} = (\sqrt{4\pi}/F_\Pi)^2$ have the same dimension [*energy*] of elementary boson fields. Their masses $M_\Pi \propto \Lambda$ and decay constants $F_\Pi \propto \Lambda$, due to the composite dynamics at the scale Λ. These LQ states have baryon number $B = 1/3$ and lepton number $L = -1$, corresponding to R_2 and $\tilde{R}_2$ states in the LQ nomenclature [160, 161], which do not suffer interference with SM processes as pointed out in [97]. The spectra in table (1), interactions (2.3), can be generalized by $\nu^e, e, u, d \to \nu^\mu, \mu, c, s$ for the second generation, and $\nu^e, e, u, d \to \nu^\tau, \tau, t, b$ for the third generation.

Although coupling G_{cut} and the composite scale Λ are unique, the coupling g_{Π_i} and mass M_{Π_i} have different values but are similar and related across generations. The main reason is that, in the four-fermion interactions, the fermion fields $\psi_{L,R}^f$ are SM gauge eigenstates. While in the ground state, they mix in different charged sectors and generations by unitary transformations $U_{L,R}^{\nu,\ell,u,d}$ [9]. Therefore, LQ states in different generations mix, provided they have the same SM charges of table 1. For example, $\Pi_a^{5/3}(\bar{e}_R u_{La})$ exhibits mixing amongst the LQ states $(\bar{\mu}_R c_{La})$ and $(\bar{\tau}_R t_{La})$. In addition to the Yukawa coupling (2.3), it can also couple to the lepton and quark in the second and third generations via flavor-mixed Yukawa couplings,

$$g_{\Pi_{5/3}}(U_R^\dagger U_L)_{1,2}(\bar{\mu}_R c_{La})\Pi_a^{-5/3} + g_{\Pi_{5/3}}(U_R^\dagger U_L)_{1,3}(\bar{\tau}_R t_{La})\Pi_a^{-5/3}, \tag{2.4}$$

where the flavor-suppressed factors $(U_R^\dagger U_L)_{1,3} < (U_R^\dagger U_L)_{1,2} < 1$ stand for the CKM-like mixing matrix elements between the first and other generations. The same discussions apply to other LQ states in table 1. Other flavor-mixed Yukawa couplings are possible, as long as they preserve SM gauge symmetries. For these reasons, LQ boson masses and Yukawa couplings should be different in generations and related by an unknown mixing matrix $(U_{L,R}^{\nu,\ell,u,d})^\dagger U_{L,R}^{\nu,\ell,u,d}$, in analogy to the CKM matrix in the quark sector and PMNS matrix in the lepton sector. We treat different composite boson masses M_{Π_i} and Yukawa couplings g_{Π_i} as theoretical parameters. The constraint $g_{\Pi_i}^2 < 8\pi/\sqrt{3}$ is inferred by studying the unitary problem [162].

These LQ bosons (table 1) and interactions (2.2)–(2.3) are the counterparts of color singlets $\Pi^{0,\pm}$ in table V and interactions (26-28) of ref. [19] by exchanging $e_{L,R} \leftrightarrow d_{L,R}^a$ and $\nu_{L,R}^e \leftrightarrow u_{L,R}^a$. The parameter spaces of Yukawa couplings g_{Π_i} and masses M_{Π_i} for investigating $\Pi^{0,\pm}$ are the same as those of LQ bosons up to the aforementioned mixing matrix elements of the order of unity. The differences are only the initial states' parton density functions (PDFs) used and the final states detected. For color singlets $\Pi^{0,\pm}$, there are decay (production) channels to (from) SM gauge bosons W, Z and γ, while color LQ states can be produced by gluon splitting or via a lepton-quark vertex. Analogously to the studies of composite fermions [19], we will discuss composite LQ fermions in a separate article, e.g. $F_R \sim \ell_R \Phi$ or $q_R \Phi$, interacting with SM gauge bosons and decaying to $\ell_R(q_R) + \Phi \to \ell_R(q_R) + \bar{\ell}_R + q_L$. We also mention the possibility of nontrivial contributions to the $B \to D^*$ anomaly $R_{D^{(*)}}$ of the charged current channel $b \to c\tau\bar{\nu}$ based on the composite boson spectra (table 1). Having the same SM charges, the state $\Pi_{u_a}^{-2/3}(\bar{u}_{Ra}\nu_L^e)$ mixes with the states $(\bar{c}_{Ra}\nu_L^\mu)$, and the state $\Pi_{d_a}^{2/3}(\bar{e}_R d_{La})$ mixes with the states $(\bar{\tau}_R b_{La})$. Therefore, we have the transition amplitude $\langle[\Pi_{u_a}^{2/3}(0)]^\dagger \Pi_{d_a}^{2/3}(x)\rangle \to (\mathcal{C}/\Lambda^2)\langle(\bar{c}_{Ra}\nu_L^\mu)(\bar{\tau}_R b_{La})\rangle$, yielding to the probability of the

flavour-changing process $b \to c\tau\bar{\nu}$, where the $\mathcal{C}$ relates to the mixing amongst quark and lepton flavours. This is similar to the discussion of the LQ scalar $R_2^{+2/3}$ ($\Pi_{d_a}^{+2/3}$) contribution to $R_{D^{(*)}}$ [163], see also [58]. We leave for a future effort the detailed analysis in this context.

3 Signal implementation and samples generation

To generate signal and background events, we utilize MadGraph5 aMC@NLO [164], incorporating the gauge (eq. (2.1)) and the contact (eq. (2.3)) interaction terms described in the previous section via the Feynrules package [165] as a Universal FeynRules Output (UFO) module [166]. Subsequently, we generate Monte Carlo (MC) samples for both the signal and SM background processes via MadGraph5 aMC@NLO, then use Pythia 8.2 [167] for including initial and final parton showering and fragmentation. The Madgraph implementation includes the b quark in our proton definition, and the interactions have been implemented up to the 3rd fermion generation with the corresponding couplings.

In this article, we consider LQs with a charge of 5/3 that couple to electron-u quark (λ_{eu}) and muon-c quark ($\lambda_{\mu c}$) pairs for the signal generation, along with an LQ with a charge of 2/3 that couples to tau-b quark ($\lambda_{\tau b}$). The signal process is generated with two types of beam hypotheses: proton-proton (pp) and photon-proton (γp). For the pp LQ production, the NNPDF31-lo-as-0118 [168] PDF is used. For the γp collisions, we choose the MRST2004qed-proton PDF [169]. This decision is motivated by our aim to distinguish between the elastic and inelastic contributions of the photon. The NNPDF set previously mentioned incorporates both the elastic and inelastic contributions (as does the LUX PDF [170]), rendering it impractical to separate the two components. The MRST2004qed PDF allows for the separation of the elastic and inelastic contributions with the configurations available in Madgraph. In our studies, we simulate the processes $pp \to \ell^+\ell^-$ plus 0, 1, 2, or at least 3 partons to incorporate the standard production modes in figure 1 (a–c) and the new production modes that are presented in the subsequent section. For the photon-induced processes, we consider $\gamma p \to \ell^+\ell^-$ plus 1 parton to focus our study on elastic versus inelastic contribution only.

The center-of-mass energy is set to 13 TeV. The values of λ vary in the range [0.5-2.5] in steps of 0.5. For the LQ masses, we consider values in the ranges (in TeV) [1.00-2.00] in steps of 0.25, [2.00, 10.00] in steps of 0.50, plus 20.00 and 30.00 TeV. Extra jets in the production of the LQ may originate from either gluons or quarks, as specified below. The former corresponds to initial or final state radiation emitted in one of the well-searched, tree-level diagrams, while the latter may give rise to novel mechanisms to generate LQs. We note that both scenarios can contribute to the overall signal, necessitating the avoidance of double counting of events among different processes. To achieve this, in the production of the signal samples, we employ the matrix-element parton shower matching technique known as MLM matching [171]. We set a matching scale of 30 GeV and ensure appropriate overlap removal in the differential jet rates of our samples. We have verified that the cross sections obtained using our implemented model are consistent within 1% with those yielded by the models LQ-UFO [172], commonly used in analyses at LHC [7], using the same generator configurations and relying on the resonant pair production mode (figure 1 (c)) that depends on α_s only.
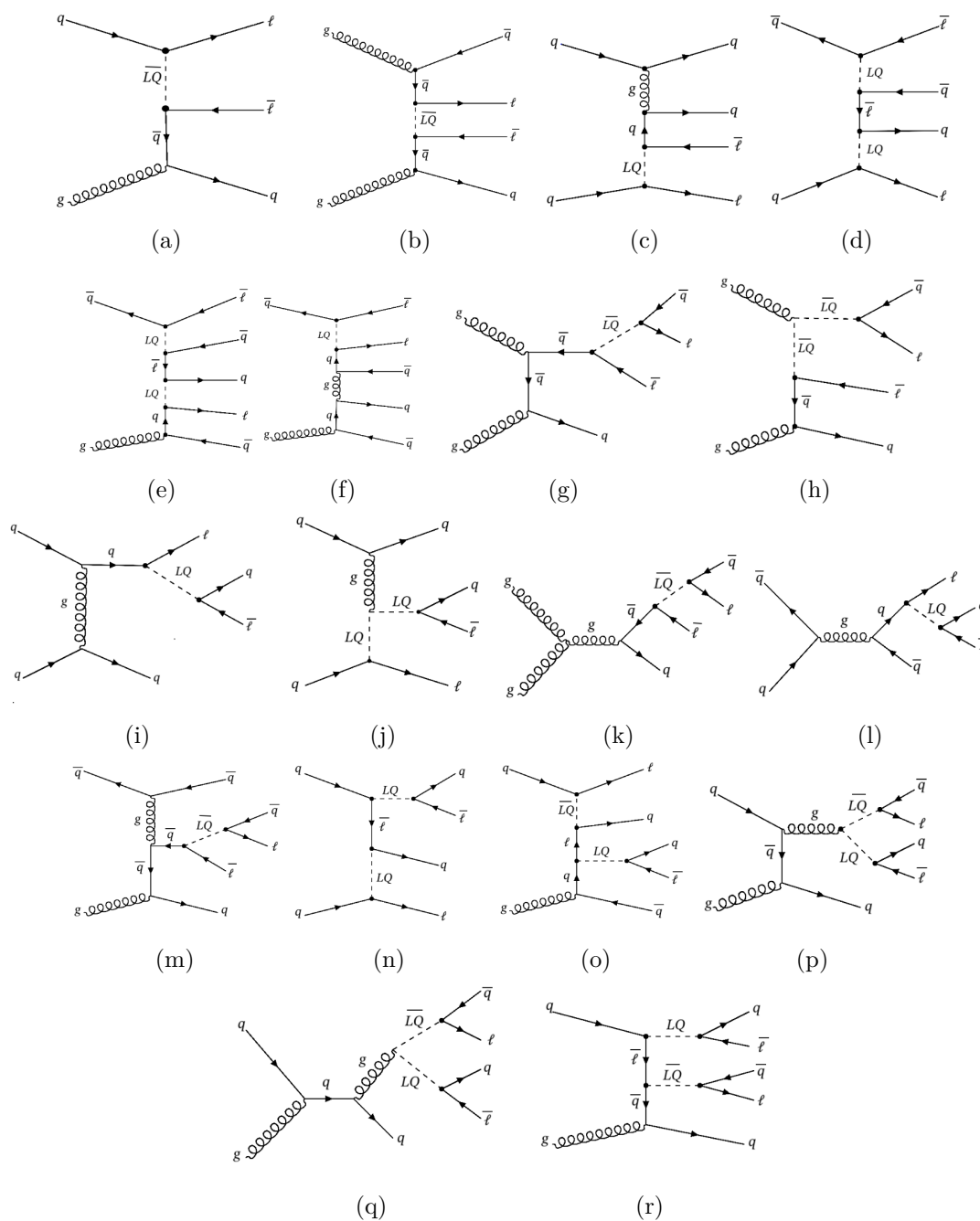
4 Exclusive LQ production

In this section, we explain LQ production in detail, emphasizing the mechanisms where LQs appear with additional jets compared to the well-established modes depicted in figure 1. We refer to this as "exclusive" LQ production, drawing an analogy to the nomenclature utilized in the study of inelastic scattering, where every reaction product is interested. Our examination of the numerous Feynman diagrams reveals three distinct cases of interest: (1) the splitting of a gluon into two quarks, one of which participates in the LQ generation, the other appearing as an additional jet; (2) the emission of a gluon from a parton that contributes to the LQ formation through separation into two quarks, with the original radiating parton and one of the gluon's quarks ending as additional jets; (3) the exchange of a lepton that may lead to up to two additional jets. We remark that, although we are highlighting these possibilities in the context of the LQ particle, they apply to any SM and BSM particle that permits the relevant couplings to quarks and leptons. It is also possible to have the emission of a gluon, arising from initial or final state radiation, that subsequently manifests as an additional jet (or two jets if it divides into quarks) and does not couple to the LQ. Although this latter occurrence also augments the jet multiplicity compared to the reference modes at the Born level, this scenario does not introduce new production processes, as it is anticipated within the hadronic environment of the LHC for any mechanism. The third instance above has been previously discussed in relation to pair production [89, 90] only, although it may occur also in t-channel and single production, and it introduces two additional new physics vertices that enhance the cross section rapidly with respect to λ. The generation of an LQ initiated via a lepton is a unique production mode, and we treat it in the next sub-section.

The t-channel process studied in literature refers to the diagram in figure 1 (a) where the LQ interacts with two valence quarks in the initial state. However, such a production mode may be induced from the initial-state gluon splitting in either one or both incoming protons, as indicated in figure 2 (a, b). Another possibility is that a gluon or a lepton is exchanged, as illustrated in figure 2 (c, d), or a combination of the previous two cases, see figure 2 (e, f). Single LQ production is displayed on the diagrams in figure 1 (b) where the LQ creation starts from a gluon and a quark. Cases of both initial gluon splitting or gluon emission from a parton are possible, as illustrated in figure 2 (g-m). Figure 2 (n, o) instead shows the case where a lepton is exchanged in the process. The quantum chromodynamic LQ pair production happens via a gluon that separates into two LQs, and the primary mode is shown in figure 1 (c). Extra jets in final states coming from two LQ decays can originate from processes like those shown in figure 2 (p, q), while an example with a lepton exchange is displayed in figure 2 (r).

The examples discussed above describe some of the possible modes to produce LQs with additional jets, and one can expect different variants allowed by crossing-symmetry of the particles involved in the interaction vertices. We note that combining the instances (1), (2), (3), as in diagram figure 2 (e,f), further increases the number of jets and such diagrams are indeed produced by MadGraph, although their production cross section decreases as the number of jets increases.

In this study, we aim to understand the impact of these processes in addition to those usually considered in traditional LHC searches. To accomplish this, we compare the cross

Figure 2. Examples of Feynman diagrams for leptoquarks originating via one of the three mechanisms highlighted in exclusive production: (i) the splitting of a gluon into two quarks, (ii) the emission of a gluon from a parton, and (iii) the exchange of a lepton. They are illustrated for t-channel (a-f), single (g-o), and pair (p-r) production of leptoquarks.

sections of the reference LQ production modes in figure 1 (b, c) with those obtained by specifying the corresponding dilepton plus jets (originating from quarks) final state that intercepts the new mechanisms described above. The t-channel process in figure 1 (a) is not considered, as it is produced with only two leptons in its traditional form. The comparison is presented in figure 3 with respect to both single (a) and pair (b) production, along with the ratio of the two production variants (c) for λ_{eu}, $\lambda_{\mu c}$, and $\lambda_{\tau b}$ equal to 1.0. These couplings encompass each fermion generation and are selected to represent all potential lepton-quark-LQ vertices. Indeed, the primary factor influencing the LQ production cross section, aside from its mass and coupling strength, is the specific quark to which it couples. Consequently, we can anticipate a comparable enhancement in the cross section for LQs coupling to other quarks, in alignment with the PDFs, as well as for couplings involving neutrinos and cross-diagonal interactions between quarks and leptons.

Our analysis reveals a significant enhancement in the cross section across all cases when incorporating the new production modes. Specifically, there is an approximately 70%, 85%, and threefold (fourfold, 2.4-fold, 75%) increase against single (pair) production of figure 1 for λ_{eu}, $\lambda_{\mu c}$, and $\lambda_{\tau b}$ set to 1 and an LQ mass of 1 TeV. This increase becomes larger at LQ mass of 3 TeV, corresponding to a factor of about 16, 17, 240 (300, 190, 170), respectively.

The observed enhancement is influenced by two factors: the flavor of the quark involved in the lepton-quark-LQ vertex according to the PDFs of the proton and the diminishing resonant single and pair production cross section as a function of LQ mass due to the kinematic limit imposed by the LHC center-of-mass energy. The former implies that the new mechanisms contribute more for lower generation quarks with respect to pair production (figure 1 (c)), which is mainly determined by gluon-gluon fusion and is independent of the quark generation, while they become more relevant for higher generation quarks against single production (figure 1 (b)) that depends on one quark and is thus reduced for higher quark generations. The latter determines the larger increase at higher LQ masses, where the probability of creating a resonant LQ becomes lower and lower, while for the non-resonant mechanisms of figure 2 such a constraint is less stringent. For completeness, we should note that the new processes introduced here rely on the presence of gluons in the protons, which taper off at higher LQ masses, where valence quarks will dominate, as will the Drell-Yan t-channel. The gain of these new mechanisms for other beyond SM (or SM) particles will vary depending on their possible production modes.

This study marks the first presentation of such an analysis in the literature, demonstrating a significant benefit from considering the aforementioned production mechanisms. Based on these findings, we propose two distinct recommendations for future experimental strategies in searches for LQs or other particles at the LHC. First, we suggest revising the current approach where searches designed to detect events with a specific final state only consider particles from the corresponding primary production mode. As an example, it is customary that searches requiring two leptons and two jets in the final state target only LQ pair production (figure 1 (c)). Our study, instead, as indicated in figures 2 and 3 for LQs, shows that the primary production modes contribute at varying jet multiplicities. Therefore, searches should be expanded to include all possible signal contributions, even if they target a single final state. Second, we remark the importance of considering t-channel contributions at any

jet multiplicity, not just figure 1 (a), by exploiting its unique topology and using angular spectra of dileptons, which outperform traditional energy-related observables in terms of sensitivity (see [85]). We will discuss in section 5 how to leverage this feature to enhance the overall search sensitivity.

As a final consideration, we address how to integrate all production modes to analyze the expected sensitivity to LQ signals at the LHC. Our focus is on an LQ with coupling $\lambda_{\mu c}$, as λ_{eu} is predominantly determined by the Drell-Yan t-channel, and $\lambda_{\tau b}$ has a more complicated nature due to the presence of a τ lepton. Simply generating LQ events separately for each jet multiplicity and adding them would result in some degree of double counting of events. Instead, we produce exclusive LQ signal incorporating a lepton pair plus 0, 1, 2, and 3 jets (a jet being either a quark or a gluon to better simulate radiation effects), simultaneously. We correct for potential double counting issues using the jet matching technique detailed in section 3. The cross sections for all relevant processes are presented in figure 4, showing that exclusive LQ production dominates and is therefore utilized for our sensitivity analysis discussed below.

4.1 Lepton initiated LQ production

The idea that LQs may be produced from a lepton that stems via vacuum fluctuations in the proton was proposed a long time ago [92]. It has become recently feasible due to an improved estimate of the lepton density functions (LDFs) [100–102] and it has been used at CMS [145]. Here, we discuss how such a process enters our view to proceed to a global search for LQs.

The first point to remark on is that the works [100–102, 145] study s-channel LQ production only. However, t-channel LQ exchange is possible and should be considered. The second aspect to note is that one can consider lepton-induced processes using the exclusive production approach introduced here by noting that all the processes illustrated in figure 2 and discussed above are equally possible by simply substituting a gluon that splits into two quarks with a photon that splits into two leptons.

There is another more general consideration to mention in relation to the lepton that produces the LQ, and it concerns whether its mother particle, the photon, for example, stems from elastic (the proton remains intact, figure 5 (a)) or inelastic (the proton does not remain intact, figure 5 (b)). For the elastic case, we define one of the protons to be a photon, while for the inelastic case, we include the photon in the proton without changing the default type. For $\lambda_{\mu c} = 1$, we see that the ratio of the contribution to the cross section from the elastic to the inelastic case is about 27%. Despite the lower ratio for the elastic case, we point out that a dedicated search relying on the elastic case would have an enormous advantage in mitigating the SM background, as pointed out in several investigations [173].

By comparing the total cross section obtained summing up both elastic and inelastic cases with that using the LDFs as in figure 1 (d), we see that the two are consistent within 20%.

5 Search strategy

The signal we look for produces a signature with two leptons in the final state plus a given number of jets (0, 1, 2, or at least 3). The samples described in section 3 for the $\lambda_{\mu c}$ coupling, as discussed in section 4, are used in the event selection. The events pass the
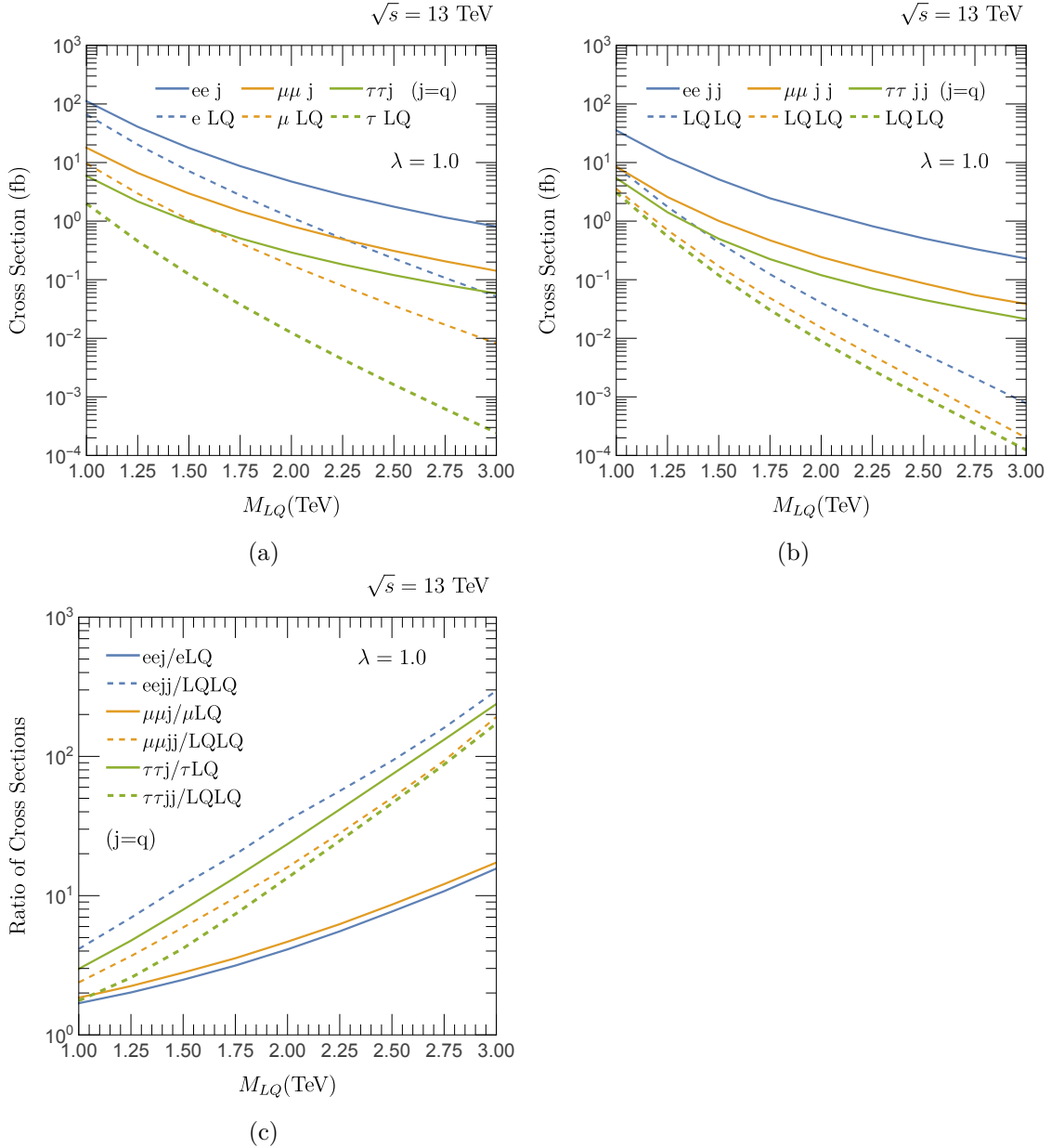
Figure 3. Comparison of cross sections versus LQ mass for single (a) and pair (b) productions of figure 1 (b, c) with those obtained by specifying the corresponding dilepton plus jets (originating from quarks) final state, along with their ratio (c) for λ_{eu}, $\lambda_{\mu c}$, and $\lambda_{\tau b}$ set to 1.0.

signal selection if they satisfy the following baseline requirements: exactly two muons with transverse momentum $p_{\mathrm{T}} > 20\,\mathrm{GeV}$, pseudorapidity $|\eta| < 2.5$, and invariant mass greater than $120\,\mathrm{GeV}$; missing transverse energy lower than $50\,\mathrm{GeV}$; and no jets originating from b quarks. We find that the selection efficiency is about 30% or higher from masses of 1 TeV and all coupling values.

Jets are chosen to have $p_{\mathrm{T}} > 20\,\mathrm{GeV}$ and $|\eta| < 5$, and to be spatially separated from the selected muons by $\Delta R > 0.4$, where $\Delta R = \sqrt{(\Delta\eta)^2 + (\Delta\phi)^2}$ and ϕ is the azimuthal angle.
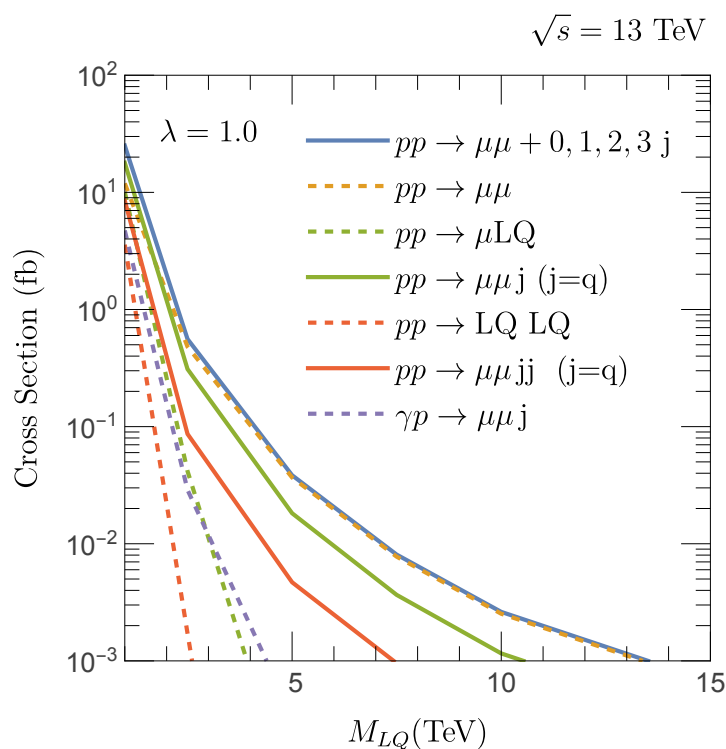
Figure 4. Cross sections for different leptoquark production modes, for a coupling of the muon to the c quark $\lambda = 1$.
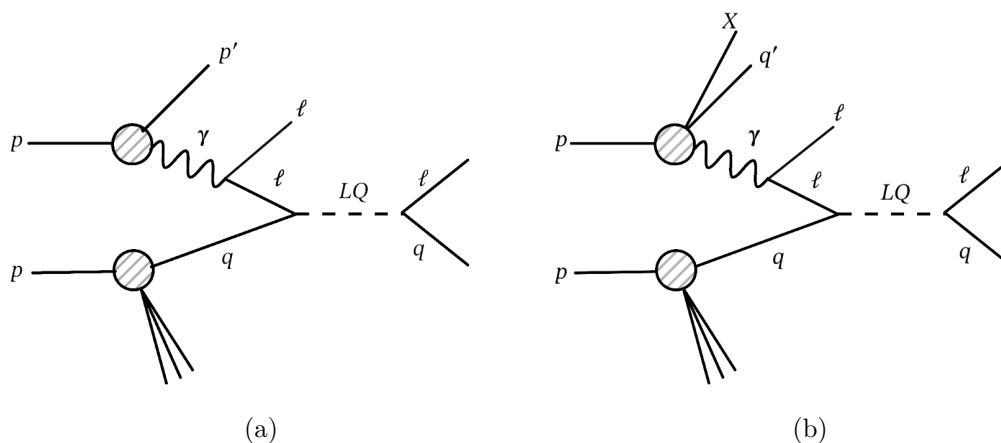
Figure 5. Feynman diagrams for the single leptoquark production for the cases where a photon that splits into two leptons is radiated by the proton elastically (a) or inelastically (b).

We do not set any condition on a minimal number of jets, as we separate the signal region events into categories with 0, 1, 2, or at least 3 jets.

As discussed in section 4, one significant finding of this study is the contribution from t-channel processes among the new mechanisms illustrated in figure 2, in addition to the Drell-Yan production depicted in figure 1. To optimize our search criteria to be sensitive to these processes, we consider angular spectra of dileptons. This method offers superior discrimination against background (see [85]) compared to methods considering the energy-related observables typically employed in LQ searches, which are instead well-suited for signal events featuring resonant LQs. Given our goal of building a comprehensive search strategy, we propose leveraging both these aspects simultaneously to enhance our sensitivity to the LQ signal.

In figure 6 we show the distribution from pp events from processes including two jets in the two-dimensional plane of χ and S_T, where $\chi = e^{|\eta_1 - \eta_2|}$ and η_1, η_2 are the pseudorapidities of the two muons, while S_T is defined as the sum of the scalar p_T of the leptons and selected jets. The plots are shown for two signal hypotheses: with leptoquark mass equal to $M_{LQ} = 2\,\mathrm{TeV}$ and coupling $\lambda_{\mu c} = 1$, plot (a), and $M_{LQ} = 4\,\mathrm{TeV}$ and coupling $\lambda_{\mu c} = 2.5$ plot (b). The SM background is shown on plot (c).

Background events are generated at leading order (LO) with PDF NNPDF31-lo-as-0118 [168], and scaled using next-to-leading-order (NLO) cross sections where appropriate. The processes we consider are W + jets ($W \to l + \nu$), Drell-Yan (charged lepton decays) + jets, single top, $t\bar{t}$, and diboson (WW, WZ, and ZZ). Background processes are generated with sufficiently high jet multiplicities to yield an accurate comparison against our targeted signal. Generator-level production is then interfaced with Pythia 8.2 [167] for parton showering and hadronization using the Monash 2013 tune [174]. Detector response simulation is obtained via the Delphes framework [175]. As in our signal events, jet matching is implemented using the MLM algorithm to avoid double counting of events after showering and hadronization.

6 Expected sensitivity at LHC and HL-LHC

The distributions of the χ and S_T variables per jet multiplicity for the events of the signal regions are used as the final discriminant between the LQ signal and the background. We sum up signal events from both the pp and γp collisions, accounting for production cross section, efficiency, and luminosity, and use a profile-binned likelihood statistical test [176] for assessing the expected signal significance. Nuisance parameters encompassing systematic uncertainties are introduced for the signal (background), incorporating log-normal priors. We follow the same prescriptions used in the published LQ searches [122, 124] and we briefly summarize them below. The uncertainties arising from the selection of the parton distribution function in the MC production is 2.8% (3.0%), while that related to additional interaction vertices in the event amount to 0.2% (1.0%). The uncertainties associated with jet and lepton energy resolution are 0.1% (1.7%) and 0.2% (5.3%), respectively. Additionally, jet and lepton energy scale uncertainties are included with values of 0.5% (0.9%) and 1.5% (2.5%). The uncertainties for leptonic reconstruction and identification efficiency stand at 3.0% and 1.3% (0.3%). For the calculation of expected significance the "Combine Tool" is used [177]. In figure 7, we present contour plots of the expected significance in the two-dimensional plane of the coupling λ and the mass of the LQ. These plots are obtained at the center-of-mass
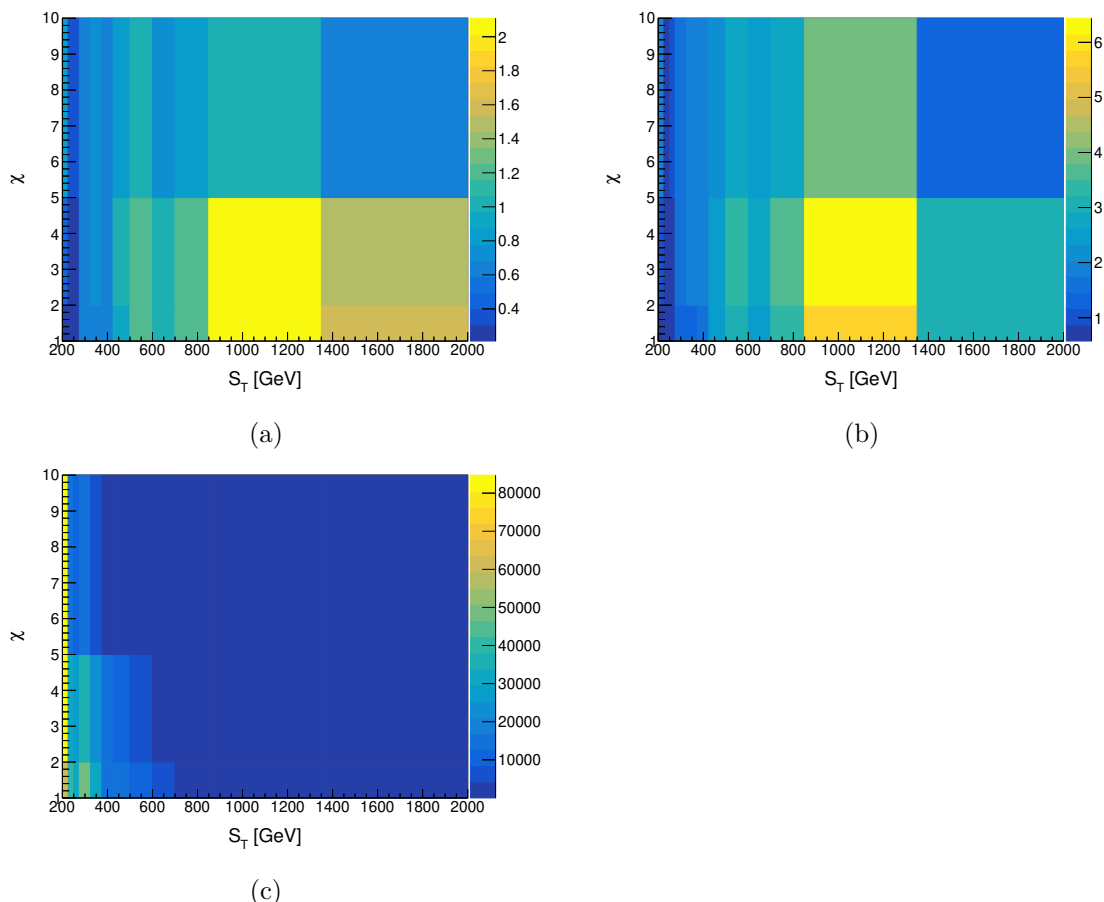
Figure 6. The plots are shown for two signal hypotheses: with leptoquark mass equal to $M_{LQ} = 2\,\mathrm{TeV}$ and coupling $\lambda_{\mu c} = 1$, plot (a), and $M_{LQ} = 4\,\mathrm{TeV}$ and coupling $\lambda_{\mu c} = 2.5$ plot (b). The SM background is shown on plot (c).

energy of $13\,\mathrm{TeV}$ and an integrated luminosity of $300\,\mathrm{fb}^{-1}$ (left), as a possible value of the luminosity expected by the end of the ongoing data-taking period at the LHC referred to as Run 3, and varying luminosity assumptions (right) at 140 (blue), 300 (red), 3000 (green) fb^{-1}, for the $5\,\sigma$ (plain line) and $2\,\sigma$ (dashed line) significance levels. The vertical lines show the most recent exclusion limits results at 95% confidence level from a search for LQs from ATLAS [112] (black dashed) and CMS [124] (violet plain) collaborations scaled for 300 (left) and 3000 (right) fb^{-1}. The results obtained with the exclusive LQ approach report a 5 (2) σ significance for LQ masses up to 2.0, 2.2, 2.5 (2.3, 2.4, 3.4) TeV, for $\lambda_{\mu c} = 0.5$, and 8.0, 9.7, 18.6 (14.9, 17.5, 27.3) TeV, for $\lambda_{\mu c} = 2.5$, at 140, 300, 3000 fb^{-1}. While ATLAS and CMS scaled results would exclude a LQ coupling to a muon–c quark pair up to masses of 1.7, 1.8, 2.2, and 1.8, 1.9, 2.3 TeV regardless of the coupling value and for the same luminosity scenarios. With the strategy developed in this article, we obtain that the $2\,\sigma$ significance with $140\,\mathrm{fb}^{-1}$ is comparable to the scaled upper limit on the LQ mass expected by ATLAS and CMS with $3000\,\mathrm{fb}^{-1}$, for the lowest coupling value that we consider.
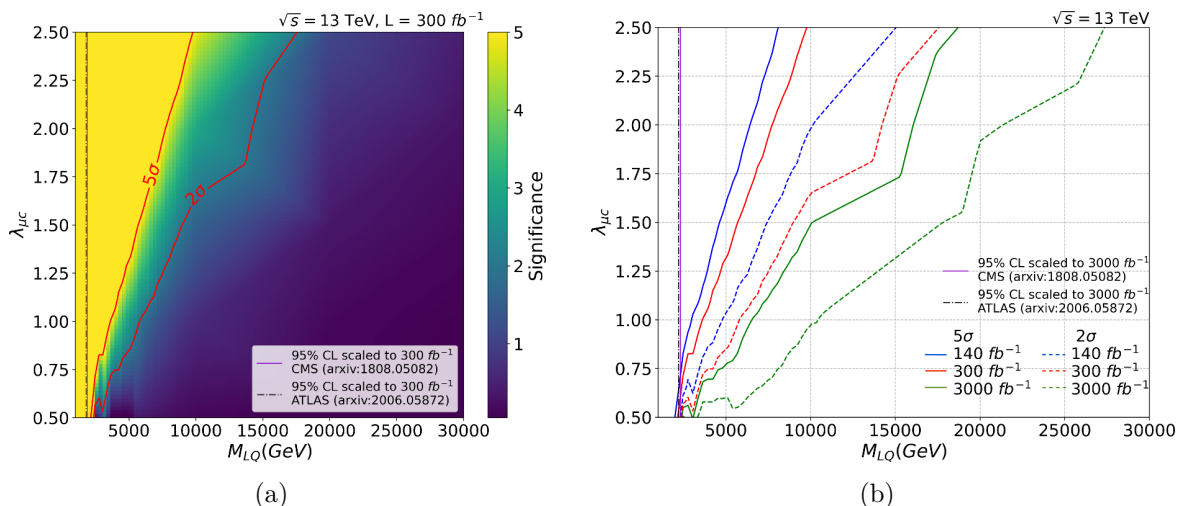
Figure 7. Signal significance in the plane of the coupling $\lambda_{\mu c}$ and the mass of the LQ using pp and γp events at $\sqrt{s} = 13$ TeV expected for 300 fb^{-1} (left) and different luminosity scenarios (right). The colored solid and dashed lines represent 5 and 2 σ levels for the analysis presented in this text, while the vertical lines show the most recent exclusion limits results at 95% confidence level from a search for LQs from ATLAS [112] (black dashed) and CMS [124] (violet plain) collaborations scaled for 300 (left) and 3000 (right) fb^{-1}.

7 Summary and remarks

As the LHC proceeds in collecting more data at the utmost center-of-mass energy and with the slow relative increase in luminosity anticipated by the High-Luminosity initiative of the accelerator, the absence of compelling evidence for new physics prompts a critical consideration. It becomes increasingly important to assess whether existing searches have thoroughly investigated all conceivable paths or whether new approaches may still be formulated to enhance the discovery potential and to unlock access to a phase space that was not considered reachable before.

In this paper, we have tackled this question by conducting a comprehensive study of the well-motivated, known, and extensively researched LQ particle. Although we carry out a study that is valid for any model, we have relied on a novel scenario of LQ composite particles via the NJL model with effective strong four-fermion couplings [10, 11]. This is an important addition to the literature, as in the event of discovering a beyond Standard Model particle consistent with an LQ, it will be crucial to ascertain its nature and determine its classification within the various discernible models. In particular, the NJL model introduces a different concept of compositeness than those considered at LHC [106, 178–184] and offers a broad variety of new composite particles: integer charge bosons $\Pi^f \sim (\bar{\psi}_R^f \psi_L^f)$ and fermions $F_R^f \sim \psi_R^f (\bar{\psi}_R^f \psi_L^f) \sim \psi_R^f \Pi^f$ [19], fractional charge bosons such as the LQ bosons studied here, composite LQ fermions, and composite Higgs to be studied in future works. These could manifest in signatures that have not yet been explored at the LHC.

Compared to existing investigations that rely on the primary LQ production modes in figure 1, for the first time, we have examined the impact on the sensitivity of the search for particles when they are produced in association with additional jets. We have found

that several new mechanisms are possible besides the classical pair, single, and Drell-Yan non-resonant LQ generation, as discussed in section 4 and illustrated in figure 2. We refer to the ensemble of all allowed processes as "exclusive" LQ production, in analogy to the terminology adopted in inelastic scattering, where all reaction products are involved.

We have observed that the exclusive cross section exceeds those of the mechanisms considered in traditional searches. These carry an increase of approximately 70%, 85%, and threefold (fourfold, 2.4-fold, 75%) over the single (pair) production modes shown in figure 1 respectively for λ_{eu}, $\lambda_{\mu c}$, and $\lambda_{\tau b}$ with their value set to 1 and an LQ mass of 1 TeV. This increase becomes larger at an LQ mass of 3 TeV, corresponding to a factor of about 16, 17, 240 (300, 190, 170), respectively for the considered couplings over single (pair) production. This result represents an outstanding gain in discovery potential due to the enhanced signal cross section. Additionally, the signal significance is further increased because, for the same primary mode, the exclusive production captures new mechanisms at higher jet multiplicities, which have been shown to further mitigate the SM background [146–153].

Given all the findings presented in this paper, we propose two fundamental recommendations for developing strategies to investigate new physics, whether for LQs or other particles. The first is the inclusion of all possible signal contributions across varying jet multiplicities, employing the exclusive approach rather than relying solely on the primary production modes, even if an analysis targets a single final state. The second is to use angular spectra in conjunction with energy-related observables to fully exploit t-channel contribution and achieve the highest significance.

Moreover, we have expanded this approach referring to LDFs and we also pursued an unprecedented distinction between inelastic and elastic modes, the former resulting in about 80% of the total although the latter would benefit from reduced background contamination [173].

Finally, we propose a global strategy as our key recommendation, to intercept t-channel, single, and pair signal generation at different jet multiplicities and simultaneously using the S_T and χ distributions. We anticipate that an optimal combination of the energetic and angular variables could be exploited by relying on machine learning techniques. As shown in figure 7, we achieve a significance of 5 (2) σ for LQ masses up to 2.0, 2.2, 2.5 (2.3, 2.4, 3.4) TeV, for $\lambda_{\mu c} = 0.5$, and 8.0, 9.7, 18.6 (14.9, 17.5, 27.3) TeV, for $\lambda_{\mu c} = 2.5$, at 140, 300, 3000 fb^{-1}. The significance of 2 σ with 140 fb^{-1} is comparable to the scaled upper limit on the LQ mass expected by ATLAS [112] and CMS [124] with 3000 fb^{-1} for the lowest coupling value that we consider.

These results are notably relevant for BSM scenarios with preferential couplings to higher fermion generations, including models that have the potential to explain some of the persistent, yet to be confirmed, anomalies in high energy physics (such as the aforementioned $B \to D^*$ and $(g-2)_\mu$ precision measurements), as they allow to probe a much wider region of the LQ coupling-mass plane compared to traditional searches and especially for couplings to higher generation fermions.

In light of the discovery potential and the results presented in this paper, we assert that an exclusive approach to LQ searches should be incorporated into future investigations at the LHC. In generalizing these results, we find that the exclusive paradigm and the aforementioned recommendations should be applied to the exploration of any new particles.

Acknowledgments

References

[1] ATLAS collaboration, *Search for new resonances in mass distributions of jet pairs using 139 fb^{-1} of pp collisions at $\sqrt{s} = 13$ TeV with the ATLAS detector*, *JHEP* **03** (2020) 145 [`arXiv:1910.08447`] [ɪɴSPIRE].

[2] ATLAS collaboration, *Search for new phenomena in pp collisions in final states with tau leptons, b-jets, and missing transverse momentum with the ATLAS detector*, *Phys. Rev. D* **104** (2021) 112005 [`arXiv:2108.07665`] [ɪɴSPIRE].

[3] ATLAS collaboration, *Search for a right-handed gauge boson decaying into a high-momentum heavy neutrino and a charged lepton in pp collisions with the ATLAS detector at $\sqrt{s} = 13$ TeV*, *Phys. Lett. B* **798** (2019) 134942 [`arXiv:1904.12679`] [ɪɴSPIRE].

[4] CMS collaboration, *Search for narrow resonances in the b-tagged dijet mass spectrum in proton-proton collisions at $\sqrt{s} = 13$ TeV*, *Phys. Rev. D* **108** (2023) 012009, all figures and tables can be found at http://cms-results.web.cern.ch/cms-results/public-results/publications/EXO-20-008 [`arXiv:2205.01835`].

[5] CMS collaboration, *Search for resonant and nonresonant new phenomena in high-mass dilepton final states at $\sqrt{s} = 13$ TeV*, *JHEP* **07** (2021) 208 [`arXiv:2103.02708`] [ɪɴSPIRE].

[6] CMS collaboration, *Search for high mass dijet resonances with a new background prediction method in proton-proton collisions at $\sqrt{s} = 13$ TeV*, *JHEP* **05** (2020) 033 [`arXiv:1911.03947`] [ɪɴSPIRE].

[7] CMS collaboration, *Search for singly and pair-produced leptoquarks coupling to third-generation fermions in proton-proton collisions at $\sqrt{s} = 13$ TeV*, *Phys. Lett. B* **819** (2021) 136446 [`arXiv:2012.04178`] [ɪɴSPIRE].

[8] CMS collaboration, *Probing heavy Majorana neutrinos and the Weinberg operator through vector boson fusion processes in proton-proton collisions at $\sqrt{s} = 13$ TeV*, *Phys. Rev. Lett.* **131** (2023) 011803, all figures and tables can be found at http://cms-results.web.cern.ch/cms-results/public-results/publications/EXO-21-003 [`arXiv:2206.08956`].

[9] S.-S. Xue, *Hierarchy spectrum of SM fermions: from top quark to electron neutrino*, *JHEP* **11** (2016) 072 [`arXiv:1605.01266`] [ɪɴSPIRE].

[10] S.-S. Xue, *An effective strong-coupling theory of composite particles in UV-domain*, *JHEP* **05** (2017) 146 [arXiv:1601.06845] [INSPIRE].

[11] S.-S. Xue, *Higgs boson origin from a gauge symmetric theory of massive composite particles and massless W± and Z0 bosons at the TeV scale*, *Nucl. Phys. B* **990** (2023) 116168 [arXiv:2210.04825] [INSPIRE].

[12] H. Kleinert and S.-S. Xue, *Composite Fermions and their Pair States in a Strongly-Coupled Fermi Liquid*, *Nucl. Phys. B* **936** (2018) 352 [arXiv:1708.04023] [INSPIRE].

[13] H.B. Nielsen and M. Ninomiya, *Absence of Neutrinos on a Lattice. 1. Proof by Homotopy Theory*, *Nucl. Phys. B* **185** (1981) 20 [*Erratum ibid.* **195** (1982) 541] [INSPIRE].

[14] H.B. Nielsen and M. Ninomiya, *No Go Theorem for Regularizing Chiral Fermions*, *Phys. Lett. B* **105** (1981) 219 [INSPIRE].

[15] H.B. Nielsen and M. Ninomiya, *Intuitive understanding of anomalies: A paradox with regularization*, *Int. J. Mod. Phys. A* **6** (1991) 2913 [INSPIRE].

[16] S.-S. Xue, *The phase structure of Einstein-Cardan theory*, *Phys. Lett. B* **665** (2008) 54 [arXiv:0804.4619] [INSPIRE].

[17] S.-S. Xue, *Quantum Regge calculus of Einstein-Cartan theory*, *Phys. Lett. B* **682** (2009) 300 [arXiv:0902.3407] [INSPIRE].

[18] S.-S. Xue, *Detailed discussions and calculations of quantum Regge calculus of Einstein-Cartan theory*, *Phys. Rev. D* **82** (2010) 064039 [arXiv:0912.2435] [INSPIRE].

[19] R. Leonardi et al., *Phenomenology at the LHC of composite particles from strongly interacting Standard Model fermions via four-fermion operators of NJL type*, *Eur. Phys. J. C* **80** (2020) 309 [arXiv:1810.11420] [INSPIRE].

[20] CMS collaboration, *Search for a heavy composite Majorana neutrino in the final state with two leptons and two quarks at $\sqrt{s} = 13$ TeV*, *Phys. Lett. B* **775** (2017) 315 [arXiv:1706.08578] [INSPIRE].

[21] S. Shakeri, F. Hajkarim and S.-S. Xue, *Shedding New Light on Sterile Neutrinos from XENON1T Experiment*, *JHEP* **12** (2020) 194 [arXiv:2008.05029] [INSPIRE].

[22] L. Pacioselli, O. Panella, M. Presilla and S.-S. Xue, *Constraints on NJL four-fermion effective interactions from neutrinoless double beta decay*, *JHEP* **11** (2023) 054 [arXiv:2304.08042] [INSPIRE].

[23] S.-S. Xue, *W boson mass tension caused by its right-handed gauge coupling at high energies?*, *Nucl. Phys. B* **985** (2022) 115992 [arXiv:2205.14957] [INSPIRE].

[24] J.C. Pati and A. Salam, *Unified Lepton-Hadron Symmetry and a Gauge Theory of the Basic Interactions*, *Phys. Rev. D* **8** (1973) 1240 [INSPIRE].

[25] J.C. Pati and A. Salam, *Lepton Number as the Fourth Color*, *Phys. Rev. D* **10** (1974) 275 [INSPIRE].

[26] H. Georgi and S.L. Glashow, *Unity of All Elementary Particle Forces*, *Phys. Rev. Lett.* **32** (1974) 438 [INSPIRE].

[27] H. Fritzsch and P. Minkowski, *Unified Interactions of Leptons and Hadrons*, *Annals Phys.* **93** (1975) 193 [INSPIRE].

[28] S.S. Gershtein, A.A. Likhoded and A.I. Onishchenko, *TeV-scale leptoquarks from GUTs/string/M-theory unification*, *Phys. Rept.* **320** (1999) 159 [INSPIRE].

[29] I. Dorsner and P. Fileviez Perez, *Unification without supersymmetry: Neutrino mass, proton decay and light leptoquarks*, *Nucl. Phys. B* **723** (2005) 53 [hep-ph/0504276] [INSPIRE].

[30] S. Dimopoulos and L. Susskind, *Mass Without Scalars*, *Nucl. Phys. B* **155** (1979) 237 [INSPIRE].

[31] S. Dimopoulos, *Technicolored Signatures*, *Nucl. Phys. B* **168** (1980) 69 [INSPIRE].

[32] E. Farhi and L. Susskind, *Technicolor*, *Phys. Rept.* **74** (1981) 277.

[33] K.D. Lane and M.V. Ramana, *Walking technicolor signatures at hadron colliders*, *Phys. Rev. D* **44** (1991) 2678 [INSPIRE].

[34] B. Schrempp and F. Schrempp, *Light leptoquarks*, *Phys. Lett. B* **153** (1985) 101 [INSPIRE].

[35] B. Gripaios, *Composite Leptoquarks at the LHC*, *JHEP* **02** (2010) 045 [arXiv:0910.1789] [INSPIRE].

[36] G.R. Farrar and P. Fayet, *Phenomenology of the Production, Decay, and Detection of New Hadronic States Associated with Supersymmetry*, *Phys. Lett. B* **76** (1978) 575 [INSPIRE].

[37] P. Ramond, *Dual Theory for Free Fermions*, *Phys. Rev. D* **3** (1971) 2415 [INSPIRE].

[38] Y.A. Golfand and E.P. Likhtman, *Extension of the Algebra of Poincare Group Generators and Violation of p Invariance*, *JETP Lett.* **13** (1971) 323 [INSPIRE].

[39] A. Neveu and J.H. Schwarz, *Factorizable dual model of pions*, *Nucl. Phys. B* **31** (1971) 86 [INSPIRE].

[40] D.V. Volkov and V.P. Akulov, *Possible universal neutrino interaction*, *JETP Lett.* **16** (1972) 438 [INSPIRE].

[41] J. Wess and B. Zumino, *A Lagrangian Model Invariant Under Supergauge Transformations*, *Phys. Lett. B* **49** (1974) 52 [INSPIRE].

[42] J. Wess and B. Zumino, *Supergauge Transformations in Four-Dimensions*, *Nucl. Phys. B* **70** (1974) 39 [INSPIRE].

[43] P. Fayet, *Supergauge Invariant Extension of the Higgs Mechanism and a Model for the electron and Its Neutrino*, *Nucl. Phys. B* **90** (1975) 104 [INSPIRE].

[44] H.P. Nilles, *Supersymmetry, Supergravity and Particle Physics*, *Phys. Rept.* **110** (1984) 1 [INSPIRE].

[45] R. Barbier et al., *R-parity violating supersymmetry*, *Phys. Rept.* **420** (2005) 1 [hep-ph/0406039] [INSPIRE].

[46] M.J. Baker et al., *The Coannihilation Codex*, *JHEP* **12** (2015) 120 [arXiv:1510.03434] [INSPIRE].

[47] BaBar collaboration, *Evidence for an excess of $\bar{B} \to D^{(*)}\tau^-\bar{\nu}_\tau$ decays*, *Phys. Rev. Lett.* **109** (2012) 101802 [arXiv:1205.5442] [INSPIRE].

[48] BaBar collaboration, *Measurement of an Excess of $\bar{B} \to D^{(*)}\tau^-\bar{\nu}_\tau$ Decays and Implications for Charged Higgs Bosons*, *Phys. Rev. D* **88** (2013) 072012 [arXiv:1303.0571] [INSPIRE].

[49] Belle collaboration, *Measurement of the branching ratio of $\bar{B} \to D^{(*)}\tau^-\bar{\nu}_\tau$ relative to $\bar{B} \to D^{(*)}\ell^-\bar{\nu}_\ell$ decays with hadronic tagging at Belle*, *Phys. Rev. D* **92** (2015) 072014 [arXiv:1507.03233] [INSPIRE].

[50] LHCb collaboration, *Measurement of the ratio of branching fractions $\mathcal{B}(\bar{B}^0 \to D^{*+}\tau^-\bar{\nu}_\tau)/\mathcal{B}(\bar{B}^0 \to D^{*+}\mu^-\bar{\nu}_\mu)$*, *Phys. Rev. Lett.* **115** (2015) 111803 [*Erratum ibid.* **115** (2015) 159901] [arXiv:1506.08614] [INSPIRE].

[51] T. Mandal, S. Mitra and S. Raz, $R_{D^{(*)}}$ *motivated* $\mathcal{S}_1$ *leptoquark scenarios: Impact of interference on the exclusion limits from LHC data*, *Phys. Rev. D* **99** (2019) 055028 [arXiv:1811.03561] [INSPIRE].

[52] B. Dumont, K. Nishiwaki and R. Watanabe, *LHC constraints and prospects for* S_1 *scalar leptoquark explaining the* $\bar{B} \to D^{(*)}\tau\bar{\nu}$ *anomaly*, *Phys. Rev. D* **94** (2016) 034001 [arXiv:1603.05248] [INSPIRE].

[53] C.-H. Chen, T. Nomura and H. Okada, *Excesses of muon* $g - 2$, $R_{D^{(*)}}$, *and* R_K *in a leptoquark model*, *Phys. Lett. B* **774** (2017) 456 [arXiv:1703.03251] [INSPIRE].

[54] R. Barbieri, C.W. Murphy and F. Senia, *B-decay Anomalies in a Composite Leptoquark Model*, *Eur. Phys. J. C* **77** (2017) 8 [arXiv:1611.04930] [INSPIRE].

[55] M. Tanaka and R. Watanabe, *New physics in the weak interaction of* $\bar{B} \to D^{(*)}\tau\bar{\nu}$, *Phys. Rev. D* **87** (2013) 034028 [arXiv:1212.1878] [INSPIRE].

[56] S. Iguro and Y. Omura, *A closer look at isodoublet vector leptoquark solution to the* $R_{D^{(*)}}$ *anomaly*, *JHEP* **11** (2023) 084 [arXiv:2306.00052] [INSPIRE].

[57] A. Crivellin, D. Müller and T. Ota, *Simultaneous explanation of* $R(D^{(*)})$ *and* $b \to s\mu^+\mu^-$: *the last scalar leptoquarks standing*, *JHEP* **09** (2017) 040 [arXiv:1703.09226] [INSPIRE].

[58] D. Buttazzo, A. Greljo, G. Isidori and D. Marzocca, *B-physics anomalies: a guide to combined explanations*, *JHEP* **11** (2017) 044 [arXiv:1706.07808] [INSPIRE].

[59] L. Di Luzio, A. Greljo and M. Nardecchia, *Gauge leptoquark as the origin of B-physics anomalies*, *Phys. Rev. D* **96** (2017) 115011 [arXiv:1708.08450] [INSPIRE].

[60] M. Bordone, C. Cornella, J. Fuentes-Martin and G. Isidori, *A three-site gauge model for flavor hierarchies and flavor anomalies*, *Phys. Lett. B* **779** (2018) 317 [arXiv:1712.01368] [INSPIRE].

[61] A. Greljo and B.A. Stefanek, *Third family quark-lepton unification at the TeV scale*, *Phys. Lett. B* **782** (2018) 131 [arXiv:1802.04274] [INSPIRE].

[62] L. Di Luzio et al., *Maximal Flavour Violation: a Cabibbo mechanism for leptoquarks*, *JHEP* **11** (2018) 081 [arXiv:1808.00942] [INSPIRE].

[63] J. Fuentes-Martín and P. Stangl, *Third-family quark-lepton unification with a fundamental composite Higgs*, *Phys. Lett. B* **811** (2020) 135953 [arXiv:2004.11376] [INSPIRE].

[64] MUON g-2 collaboration, *Measurement of the Positive Muon Anomalous Magnetic Moment to 0.46 ppm*, *Phys. Rev. Lett.* **126** (2021) 141801 [arXiv:2104.03281] [INSPIRE].

[65] MUON g-2 collaboration, *Final Report of the Muon E821 Anomalous Magnetic Moment Measurement at BNL*, *Phys. Rev. D* **73** (2006) 072003 [hep-ex/0602035] [INSPIRE].

[66] M. Bauer and M. Neubert, *Minimal Leptoquark Explanation for the* $R_{D^{(*)}}$, R_K , *and* $(g - 2)_\mu$ *Anomalies*, *Phys. Rev. Lett.* **116** (2016) 141802 [arXiv:1511.01900] [INSPIRE].

[67] A. Greljo, P. Stangl and A.E. Thomsen, *A model of muon anomalies*, *Phys. Lett. B* **820** (2021) 136554 [arXiv:2103.13991] [INSPIRE].

[68] M. Du, J. Liang, Z. Liu and V.Q. Tran, *A vector leptoquark interpretation of the muon* $g - 2$ *and B anomalies*, arXiv:2104.05685.

[69] S. Parashar et al., *Phenomenology of scalar leptoquarks at the LHC in explaining the radiative neutrino masses, muon g-2, and lepton flavor violating observables*, *Phys. Rev. D* **106** (2022) 095040 [arXiv:2209.05890] [INSPIRE].

[70] S.-L. Chen, W.-W. Jiang and Z.-K. Liu, *Combined explanations of B-physics anomalies,* $(g-2)_{e,\mu}$ *and neutrino masses by scalar leptoquarks,* *Eur. Phys. J. C* **82** (2022) 959 [arXiv:2205.15794] [INSPIRE].

[71] T.A. Chowdhury and S. Saad, *Leptoquark-vectorlike quark model for the CDF* m_W, $(g-2)_\mu$, R_{K^*} *anomalies, and neutrino masses,* *Phys. Rev. D* **106** (2022) 055017 [arXiv:2205.03917] [INSPIRE].

[72] S.-P. He, *Leptoquark and vector-like quark extended model for simultaneousexplanation of W boson mass and muon* $g-2$ *anomalies,* *Chin. Phys. C* **47** (2023) 043102 [arXiv:2205.02088] [INSPIRE].

[73] K. Cheung, W.-Y. Keung and P.-Y. Tseng, *Isodoublet vector leptoquark solution to the muon* $g-2$, R_{K,K^*}, R_{D,D^*}, *and W-mass anomalies,* *Phys. Rev. D* **106** (2022) 015029 [arXiv:2204.05942] [INSPIRE].

[74] S.-P. He, *Leptoquark and vectorlike quark extended models as the explanation of the muon* $g-2$ *anomaly,* *Phys. Rev. D* **105** (2022) 035017 [*Erratum ibid.* **106** (2022) 039901] [arXiv:2112.13490] [INSPIRE].

[75] I. Bigaran and R.R. Volkas, *Reflecting on chirality: CP-violating extensions of the single scalar-leptoquark solutions for the* $(g-2)_{e,\mu}$ *puzzles and their implications for lepton EDMs,* *Phys. Rev. D* **105** (2022) 015002 [arXiv:2110.03707] [INSPIRE].

[76] X. Wang, *Muon* $(g-2)$ *and flavor puzzles in the* $U(1)_X$*-gauged leptoquark model,* *JHEP* **08** (2022) 243 [arXiv:2108.01279] [INSPIRE].

[77] D. Zhang, *Radiative neutrino masses, lepton flavor mixing and muon* $g-2$ *in a leptoquark model,* *JHEP* **07** (2021) 069 [arXiv:2105.08670] [INSPIRE].

[78] P. Fileviez Perez, C. Murgui and A.D. Plascencia, *Leptoquarks and matter unification: Flavor anomalies and the muon* $g-2$, *Phys. Rev. D* **104** (2021) 035041 [arXiv:2104.11229] [INSPIRE].

[79] K. Ban et al., *A comprehensive study of the vector leptoquark with* $U(1)_{B_3-L_2}$ *on the B-meson and muon* $g-2$ *anomalies,* *PTEP* **2023** (2023) 013B01 [arXiv:2104.06656] [INSPIRE].

[80] E. Coluccio Leskow, G. D'Ambrosio, A. Crivellin and D. Müller, $(g-2)\mu$, *lepton flavor violation, and Z decays with leptoquarks: Correlations and future prospects,* *Phys. Rev. D* **95** (2017) 055018 [arXiv:1612.06858] [INSPIRE].

[81] A. Crivellin, D. Mueller and F. Saturnino, *Correlating* $h \to \mu^+\mu^-$ *to the Anomalous Magnetic Moment of the Muon via Leptoquarks,* *Phys. Rev. Lett.* **127** (2021) 021801 [arXiv:2008.02643] [INSPIRE].

[82] R. Pohl et al., *The size of the proton,* *Nature* **466** (2010) 213 [INSPIRE].

[83] C.S. Wood et al., *Measurement of parity nonconservation and an anapole moment in cesium,* *Science* **275** (1997) 1759 [INSPIRE].

[84] I. Dorsner, S. Fajfer and A. Greljo, *Cornering Scalar Leptoquarks at LHC,* *JHEP* **10** (2014) 154 [arXiv:1406.4831] [INSPIRE].

[85] CMS collaboration, *Search for a third-generation leptoquark coupled to a* τ *lepton and a b quark through single, pair, and nonresonant production in proton-proton collisions at* $\sqrt{s} = 13$ *TeV,* *JHEP* **05** (2024) 311 [arXiv:2308.07826] [INSPIRE].

[86] ATLAS collaboration, *Search for leptoquarks decaying into the* $b\tau$ *final state in pp collisions at* $\sqrt{s} = 13$ *TeV with the ATLAS detector,* *JHEP* **10** (2023) 001 [arXiv:2305.15962] [INSPIRE].

[87] B. Diaz, M. Schmaltz and Y.-M. Zhong, *The leptoquark Hunter's guide: Pair production*, *JHEP* **10** (2017) 097 [arXiv:1706.05033] [inSPIRE].

[88] J. Blumlein, E. Boos and A. Kryukov, *Leptoquark pair production in hadronic interactions*, *Z. Phys. C* **76** (1997) 137 [hep-ph/9610408] [inSPIRE].

[89] I. Doršner, A. Lejlić and S. Saad, *Asymmetric leptoquark pair production at LHC*, *JHEP* **03** (2023) 025 [arXiv:2210.11004] [inSPIRE].

[90] I. Doršner, S. Fajfer and A. Lejlić, *Novel Leptoquark Pair Production at LHC*, *JHEP* **05** (2021) 167 [arXiv:2103.11702] [inSPIRE].

[91] C. Borschensky, B. Fuks, A. Jueid and A. Kulesza, *Scalar leptoquarks at the LHC and flavour anomalies: a comparison of pair-production modes at NLO-QCD*, *JHEP* **11** (2022) 006 [arXiv:2207.02879] [inSPIRE].

[92] J. Ohnemus, S. Rudaz, T.F. Walsh and P.M. Zerwas, *Single leptoquark production at hadron colliders*, *Phys. Lett. B* **334** (1994) 203 [hep-ph/9406235] [inSPIRE].

[93] T. Mandal, S. Mitra and S. Seth, *Single Productions of Colored Particles at the LHC: An Example with Scalar Leptoquarks*, *JHEP* **07** (2015) 028 [arXiv:1503.04689] [inSPIRE].

[94] N. Raj, *Anticipating nonresonant new physics in dilepton angular spectra at the LHC*, *Phys. Rev. D* **95** (2017) 015011 [arXiv:1610.03795] [inSPIRE].

[95] U. Haisch, L. Schnell and S. Schulte, *On Drell-Yan production of scalar leptoquarks coupling to heavy-quark flavours*, *JHEP* **11** (2022) 106 [arXiv:2207.00356] [inSPIRE].

[96] U. Haisch, L. Schnell and S. Schulte, *Drell-Yan production in third-generation gauge vector leptoquark models at NLO+PS in QCD*, *JHEP* **02** (2023) 070 [arXiv:2209.12780] [inSPIRE].

[97] S. Bansal et al., *Hunting leptoquarks in monolepton searches*, *Phys. Rev. D* **98** (2018) 015037 [arXiv:1806.02370] [inSPIRE].

[98] M. Schmaltz and Y.-M. Zhong, *The leptoquark Hunter's guide: large coupling*, *JHEP* **01** (2019) 132 [arXiv:1810.10017] [inSPIRE].

[99] A. Greljo and N. Selimovic, *Lepton-Quark Fusion at Hadron Colliders, precisely*, *JHEP* **03** (2021) 279 [arXiv:2012.02092] [inSPIRE].

[100] L. Buonocore et al., *Lepton-Quark Collisions at the Large Hadron Collider*, *Phys. Rev. Lett.* **125** (2020) 231804 [arXiv:2005.06475] [inSPIRE].

[101] L. Buonocore et al., *Resonant leptoquark at NLO with POWHEG*, *JHEP* **11** (2022) 129 [arXiv:2209.02599] [inSPIRE].

[102] A. Korajac, P. Krack and N. Selimovic, *Third-family lepton-quark fusion*, *Eur. Phys. J. C* **84** (2024) 304 [arXiv:2311.13635] [inSPIRE].

[103] A. Flórez et al., *On the sensitivity reach of LQ production with preferential couplings to third generation fermions at the LHC*, *Eur. Phys. J. C* **83** (2023) 1023 [arXiv:2307.11070] [inSPIRE].

[104] A. Crivellin and L. Schnell, *Complete Lagrangian and set of Feynman rules for scalar leptoquarks*, *Comput. Phys. Commun.* **271** (2022) 108188 [arXiv:2105.04844] [inSPIRE].

[105] ATLAS collaboration, *Search for leptoquark pair production decaying into $te^-\bar{t}e^+$ or $t\mu^-\bar{t}\mu^+$ in multi-lepton final states in pp collisions at 13 TeV with the ATLAS detector*, arXiv:2306.17642 [CERN-EP-2023-087].

[106] ATLAS collaboration, *Search for excited τ-leptons and leptoquarks in the final state with τ-leptons and jets in pp collisions at $\sqrt{s} = 13$ TeV with the ATLAS detector*, *JHEP* **06** (2023) 199 [arXiv:2303.09444] [INSPIRE].

[107] ATLAS collaboration, *Search for pair production of third-generation leptoquarks decaying into a bottom quark and a τ-lepton with the ATLAS detector*, *Eur. Phys. J. C* **83** (2023) 1075 [arXiv:2303.01294] [INSPIRE].

[108] ATLAS collaboration, *Search for pair-produced scalar and vector leptoquarks decaying into third-generation quarks and first- or second-generation leptons in pp collisions with the ATLAS detector*, *JHEP* **06** (2023) 188 [arXiv:2210.04517] [INSPIRE].

[109] ATLAS collaboration, *Search for new phenomena in final states with b-jets and missing transverse momentum in $\sqrt{s} = 13$ TeV pp collisions with the ATLAS detector*, *JHEP* **05** (2021) 093 [arXiv:2101.12527] [INSPIRE].

[110] ATLAS collaboration, *Search for pair production of third-generation scalar leptoquarks decaying into a top quark and a τ-lepton in pp collisions at $\sqrt{s} = 13$ TeV with the ATLAS detector*, *JHEP* **06** (2021) 179 [arXiv:2101.11582] [INSPIRE].

[111] ATLAS collaboration, *Search for pair production of scalar leptoquarks decaying into first- or second-generation leptons and top quarks in proton–proton collisions at $\sqrt{s} = 13$ TeV with the ATLAS detector*, *Eur. Phys. J. C* **81** (2021) 313 [arXiv:2010.02098] [INSPIRE].

[112] ATLAS collaboration, *Search for pairs of scalar leptoquarks decaying into quarks and electrons or muons in $\sqrt{s} = 13$ TeV pp collisions with the ATLAS detector*, *JHEP* **10** (2020) 112 [arXiv:2006.05872] [INSPIRE].

[113] ATLAS collaboration, *Search for a scalar partner of the top quark in the all-hadronic $t\bar{t}$ plus missing transverse momentum final state at $\sqrt{s} = 13$ TeV with the ATLAS detector*, *Eur. Phys. J. C* **80** (2020) 737 [arXiv:2004.14060] [INSPIRE].

[114] ATLAS collaboration, *Searches for third-generation scalar leptoquarks in $\sqrt{s} = 13$ TeV pp collisions with the ATLAS detector*, *JHEP* **06** (2019) 144 [arXiv:1902.08103] [INSPIRE].

[115] ATLAS collaboration, *Searches for scalar leptoquarks and differential cross-section measurements in dilepton-dijet events in proton-proton collisions at a centre-of-mass energy of $\sqrt{s} = 13$ TeV with the ATLAS experiment*, *Eur. Phys. J. C* **79** (2019) 733 [arXiv:1902.00377] [INSPIRE].

[116] ATLAS collaboration, *Search for scalar leptoquarks in pp collisions at $\sqrt{s} = 13$ TeV with the ATLAS experiment*, *New J. Phys.* **18** (2016) 093016 [arXiv:1605.06035] [INSPIRE].

[117] ATLAS collaboration, *Searches for scalar leptoquarks in pp collisions at $\sqrt{s} = 8$ TeV with the ATLAS detector*, *Eur. Phys. J. C* **76** (2016) 5 [arXiv:1508.04735] [INSPIRE].

[118] ATLAS collaboration, *Search for third generation scalar leptoquarks in pp collisions at $\sqrt{s} = 7$ TeV with the ATLAS detector*, *JHEP* **06** (2013) 033 [arXiv:1303.0526] [INSPIRE].

[119] ATLAS collaboration, *Search for second generation scalar leptoquarks in pp collisions at $\sqrt{s} = 7$ TeV with the ATLAS detector*, *Eur. Phys. J. C* **72** (2012) 2151 [arXiv:1203.3172] [INSPIRE].

[120] ATLAS collaboration, *Search for first generation scalar leptoquarks in pp collisions at $\sqrt{s} = 7$ TeV with the ATLAS detector*, *Phys. Lett. B* **709** (2012) 158 [arXiv:1112.4828] [INSPIRE].

[121] ATLAS collaboration, *Search for pair production of first or second generation leptoquarks in proton-proton collisions at $\sqrt{s} = 7$ TeV using the ATLAS detector at the LHC*, *Phys. Rev. D* **83** (2011) 112006 [arXiv:1104.4481] [INSPIRE].

[122] CMS collaboration, *Search for pair production of first-generation scalar leptoquarks at $\sqrt{s} = 13$ TeV*, *Phys. Rev. D* **99** (2019) 052002 [arXiv:1811.01197] [INSPIRE].

[123] CMS collaboration, *Inclusive nonresonant multilepton probes of new phenomena at $\sqrt{s} = 13$ TeV*, *Phys. Rev. D* **105** (2022) 112007 [arXiv:2202.08676] [INSPIRE].

[124] CMS collaboration, *Search for pair production of second-generation leptoquarks at $\sqrt{s} = 13$ TeV*, *Phys. Rev. D* **99** (2019) 032014 [arXiv:1808.05082] [INSPIRE].

[125] CMS collaboration, *Search for leptoquarks coupled to third-generation quarks in proton-proton collisions at $\sqrt{s} = 13$ TeV*, *Phys. Rev. Lett.* **121** (2018) 241802 [arXiv:1809.05558] [INSPIRE].

[126] CMS collaboration, *Search for heavy neutrinos and third-generation leptoquarks in hadronic states of two τ leptons and two jets in proton-proton collisions at $\sqrt{s} = 13$ TeV*, *JHEP* **03** (2019) 170 [arXiv:1811.00806] [INSPIRE].

[127] CMS collaboration, *Searches for physics beyond the standard model with the M_{T2} variable in hadronic final states with and without disappearing tracks in proton-proton collisions at $\sqrt{s} = 13$ TeV*, *Eur. Phys. J. C* **80** (2020) 3 [arXiv:1909.03460] [INSPIRE].

[128] CMS collaboration, *Search for dark matter in events with a leptoquark and missing transverse momentum in proton-proton collisions at 13 TeV*, *Phys. Lett. B* **795** (2019) 76 [arXiv:1811.10151] [INSPIRE].

[129] CMS collaboration, *Search for third-generation scalar leptoquarks and heavy right-handed neutrinos in final states with two tau leptons and two jets in proton-proton collisions at $\sqrt{s} = 13$ TeV*, *JHEP* **07** (2017) 121 [arXiv:1703.03995] [INSPIRE].

[130] CMS collaboration, *Search for heavy neutrinos or third-generation leptoquarks in final states with two hadronically decaying τ leptons and two jets in proton-proton collisions at $\sqrt{s} = 13$ TeV*, *JHEP* **03** (2017) 077 [arXiv:1612.01190] [INSPIRE].

[131] CMS collaboration, *Search for pair production of first and second generation leptoquarks in proton-proton collisions at $\sqrt{s} = 8$ TeV*, *Phys. Rev. D* **93** (2016) 032004 [arXiv:1509.03744] [INSPIRE].

[132] CMS collaboration, *Search for third-generation scalar Leptoquarks in the $t\tau$ channel in proton-proton collisions at $\sqrt{s} = 8$ TeV*, *JHEP* **07** (2015) 042.

[133] CMS collaboration, *Search for pair production of third-generation scalar leptoquarks and top squarks in proton–proton collisions at $\sqrt{s} = 8$ TeV*, *Phys. Lett. B* **739** (2014) 229 [arXiv:1408.0806] [INSPIRE].

[134] CMS collaboration, *Search for third-generation leptoquarks and scalar bottom quarks in pp collisions at $\sqrt{s} = 7$ TeV*, *JHEP* **12** (2012) 055 [arXiv:1210.5627] [INSPIRE].

[135] CMS collaboration, *Search for pair production of first- and second-generation scalar leptoquarks in pp collisions at $\sqrt{s} = 7$ TeV*, *Phys. Rev. D* **86** (2012) 052013 [arXiv:1207.5406] [INSPIRE].

[136] CMS collaboration, *Search for first generation scalar leptoquarks in the $e\nu jj$ channel in pp collisions at $\sqrt{s} = 7$ TeV*, *Phys. Lett. B* **703** (2011) 246 [arXiv:1105.5237] [INSPIRE].

[137] CMS collaboration, *Search for pair production of second-generation scalar leptoquarks in pp collisions at $\sqrt{s} = 7$ TeV*, *Phys. Rev. Lett.* **106** (2011) 201803 [arXiv:1012.4033] [INSPIRE].

[138] CMS collaboration, *Search for pair production of first-generation scalar leptoquarks in pp collisions at $\sqrt{s} = 7$ TeV*, *Phys. Rev. Lett.* **106** (2011) 201802 [arXiv:1012.4031] [INSPIRE].

[139] ATLAS collaboration, *A search for an unexpected asymmetry in the production of $e^+\mu^-$ and $e^-\mu^+$ pairs in proton-proton collisions recorded by the ATLAS detector at $\sqrt{s} = 13$ TeV*, *Phys. Lett. B* **830** (2022) 137106 [arXiv:2112.08090] [INSPIRE].

[140] CMS collaboration, *Search for single production of scalar leptoquarks in proton-proton collisions at $\sqrt{s} = 8\,TeV$*, *Phys. Rev. D* **93** (2016) 032005 [*Erratum ibid.* **95** (2017) 039906] [arXiv:1509.03750] [INSPIRE].

[141] CMS collaboration, *Search for a singly produced third-generation scalar leptoquark decaying to a τ lepton and a bottom quark in proton-proton collisions at $\sqrt{s} = 13$ TeV*, *JHEP* **07** (2018) 115 [arXiv:1806.03472] [INSPIRE].

[142] CMS collaboration, *Search for new particles in events with energetic jets and large missing transverse momentum in proton-proton collisions at $\sqrt{s} = 13$ TeV*, *JHEP* **11** (2021) 153 [arXiv:2107.13021] [INSPIRE].

[143] CMS collaboration et al., *Search for a third-generation leptoquark coupled to a τ lepton and a b quark through single, pair and nonresonant production at $\sqrt{s} = 13$ TeV*, *JHEP* **05** (2024) 311 [arXiv:2308.07826].

[144] CMS collaboration, *Search for new physics in the τ lepton plus missing transverse momentum final state in proton-proton collisions at $\sqrt{s} = 13$ TeV*, *JHEP* **09** (2023) 051 [arXiv:2212.12604] [INSPIRE].

[145] CMS collaboration, *Search for Scalar Leptoquarks Produced via τ-Lepton–Quark Scattering in pp Collisions at $\sqrt{s} = 13$ TeV*, *Phys. Rev. Lett.* **132** (2024) 061801 [arXiv:2308.06143] [INSPIRE].

[146] CMS collaboration, *Search for a high-mass dimuon resonance produced in association with b quark jets at $\sqrt{s} = 13$ TeV*, *JHEP* **10** (2023) 043 [arXiv:2307.08708] [INSPIRE].

[147] ATLAS collaboration, *Search for new phenomena in final states with two leptons and one or no b-tagged jets at $\sqrt{s} = 13$ TeV using the ATLAS detector*, *Phys. Rev. Lett.* **127** (2021) 141801 [arXiv:2105.13847] [INSPIRE].

[148] ATLAS collaboration, *Search for scalar resonances decaying into $\mu^+\mu^-$ in events with and without b-tagged jets produced in proton-proton collisions at $\sqrt{s} = 13$ TeV with the ATLAS detector*, *JHEP* **07** (2019) 117 [arXiv:1901.08144] [INSPIRE].

[149] CMS collaboration, *Search for MSSM Higgs bosons decaying to $\mu^+\mu^-$ in proton-proton collisions at $\sqrt{s} = 13$ TeV*, *Phys. Lett. B* **798** (2019) 134992 [arXiv:1907.03152] [INSPIRE].

[150] M. Abdullah et al., *Probing a simplified, W' model of $R(D^{(*)})$ anomalies using b-tags, τ leptons and missing energy*, *Phys. Rev. D* **98** (2018) 055016 [arXiv:1805.01869] [INSPIRE].

[151] M. Abdullah et al., *Bottom-quark fusion processes at the LHC for probing Z' models and B-meson decay anomalies*, *Phys. Rev. D* **97** (2018) 075035 [arXiv:1707.07016] [INSPIRE].

[152] D. Barbosa et al., *Probing a Z' with non-universal fermion couplings through top quark fusion, decays to bottom quarks, and machine learning techniques*, *Eur. Phys. J. C* **83** (2023) 413 [arXiv:2210.15813] [INSPIRE].

[153] M. Abdullah et al., *A heavy neutral gauge boson near the Z boson mass pole via third generation fermions at the LHC*, *Phys. Lett. B* **803** (2020) 135326 [arXiv:1912.00102] [INSPIRE].

[154] S.-S. Xue, *A possible scaling region of chiral fermions on a lattice*, *Nucl. Phys. B* **486** (1997) 282 [`hep-lat/9605005`] [ɪɴSPIRE].

[155] S.-S. Xue, *Chiral gauged fermions on a lattice*, *Nucl. Phys. B* **580** (2000) 365 [`hep-lat/0002026`] [ɪɴSPIRE].

[156] S.-S. Xue, *A further study of the possible scaling region of lattice chiral fermions*, *Phys. Rev. D* **61** (2000) 054502 [`hep-lat/9910013`] [ɪɴSPIRE].

[157] S.-S. Xue, *Ultraviolet fixed point and massive composite particles in TeV scales*, *Phys. Lett. B* **737** (2014) 172 [`arXiv:1405.1867`] [ɪɴSPIRE].

[158] W.A. Bardeen, C.T. Hill and M. Lindner, *Minimal Dynamical Symmetry Breaking of the Standard Model*, *Phys. Rev. D* **41** (1990) 1647 [ɪɴSPIRE].

[159] S.-S. Xue, *Higgs Boson and Top-Quark Masses and Parity-Symmetry Restoration*, *Phys. Lett. B* **727** (2013) 308 [`arXiv:1308.6486`] [ɪɴSPIRE].

[160] I. Doršner et al., *Physics of leptoquarks in precision experiments and at particle colliders*, *Phys. Rept.* **641** (2016) 1 [`arXiv:1603.04993`] [ɪɴSPIRE].

[161] I. Doršner and A. Greljo, *Leptoquark toolbox for precision collider studies*, *JHEP* **05** (2018) 126 [`arXiv:1801.07641`] [ɪɴSPIRE].

[162] L. Di Luzio and M. Nardecchia, *What is the scale of new physics behind the B-flavour anomalies?*, *Eur. Phys. J. C* **77** (2017) 536 [`arXiv:1706.01868`] [ɪɴSPIRE].

[163] A. Angelescu et al., *Single leptoquark solutions to the B-physics anomalies*, *Phys. Rev. D* **104** (2021) 055017 [`arXiv:2103.12504`] [ɪɴSPIRE].

[164] J. Alwall et al., *MadGraph 5: Going Beyond*, *JHEP* **06** (2011) 128 [`arXiv:1106.0522`] [ɪɴSPIRE].

[165] A. Alloul et al., *FeynRules 2.0 - A complete toolbox for tree-level phenomenology*, *Comput. Phys. Commun.* **185** (2014) 2250 [`arXiv:1310.1921`] [ɪɴSPIRE].

[166] C. Degrande et al., *UFO - The Universal FeynRules Output*, *Comput. Phys. Commun.* **183** (2012) 1201 [`arXiv:1108.2040`] [ɪɴSPIRE].

[167] T. Sjöstrand et al., *An introduction to PYTHIA 8.2*, *Comput. Phys. Commun.* **191** (2015) 159 [`arXiv:1410.3012`] [ɪɴSPIRE].

[168] NNPDF collaboration, *Parton distributions from high-precision collider data*, *Eur. Phys. J. C* **77** (2017) 663 [`arXiv:1706.00428`] [ɪɴSPIRE].

[169] A.D. Martin, R.G. Roberts, W.J. Stirling and R.S. Thorne, *Parton distributions incorporating QED contributions*, *Eur. Phys. J. C* **39** (2005) 155 [`hep-ph/0411040`] [ɪɴSPIRE].

[170] NNPDF collaboration, *Illuminating the photon content of the proton within a global PDF analysis*, *SciPost Phys.* **5** (2018) 008 [`arXiv:1712.07053`] [ɪɴSPIRE].

[171] M.L. Mangano, M. Moretti, F. Piccinini and M. Treccani, *Matching matrix elements and shower evolution for top-quark production in hadronic collisions*, *JHEP* **01** (2007) 013 [`hep-ph/0611129`] [ɪɴSPIRE].

[172] LQ UFO, *CMS-project-generators*, https://cms-project-generators.web.cern.ch/cms-project-generators/LQ_UFO.tar.gz.

[173] TOTEM and CMS collaborations, *First Search for Exclusive Diphoton Production at High Mass with Tagged Protons in Proton-Proton Collisions at $\sqrt{s} = 13$ TeV*, *Phys. Rev. Lett.* **129** (2022) 011801 [`arXiv:2110.05916`] [ɪɴSPIRE].

[174] P. Skands, S. Carrazza and J. Rojo, *Tuning PYTHIA 8.1: the Monash 2013 Tune*, *Eur. Phys. J. C* **74** (2014) 3024 [arXiv:1404.5630] [ɪɴSPIRE].

[175] DELPHES 3 collaboration, *DELPHES 3, A modular framework for fast simulation of a generic collider experiment*, *JHEP* **02** (2014) 057 [arXiv:1307.6346] [ɪɴSPIRE].

[176] Particle Data Group, *Statistics*, (2021), https://pdg.lbl.gov/.

[177] CMS collaboration, *The CMS Statistical Analysis and Combination Tool: COMBINE*, arXiv:2404.06614 [ɪɴSPIRE].

[178] ATLAS collaboration, *Search for excited electrons singly produced in proton-proton collisions at $\sqrt{s} = 13$ TeV with the ATLAS experiment at the LHC*, *Eur. Phys. J. C* **79** (2019) 803 [arXiv:1906.03204] [ɪɴSPIRE].

[179] ATLAS collaboration, *Search for new phenomena in high-mass final states with a photon and a jet from pp collisions at $\sqrt{s} = 13$ TeV with the ATLAS detector*, *Eur. Phys. J. C* **78** (2018) 102 [arXiv:1709.10440] [ɪɴSPIRE].

[180] CMS collaboration, *Search for contact interactions and large extra dimensions in the dilepton mass spectra from proton-proton collisions at $\sqrt{s} = 13$ TeV*, *JHEP* **04** (2019) 114 [arXiv:1812.10443] [ɪɴSPIRE].

[181] CMS collaboration, *Search for an excited lepton that decays via a contact interaction to a lepton and two jets in proton-proton collisions at $\sqrt{s} = 13$ TeV*, *JHEP* **05** (2020) 052 [arXiv:2001.04521] [ɪɴSPIRE].

[182] CMS collaboration, *Search for a heavy composite Majorana neutrino in events with dilepton signatures from proton-proton collisions at $\sqrt{s} = 13$ TeV*, *Phys. Lett. B* **843** (2023) 137803 [arXiv:2210.03082] [ɪɴSPIRE].

[183] CMS collaboration, *Search for excited leptons in $\ell\ell\gamma$ final states in proton-proton collisions at $\sqrt{s} = 13$ TeV*, *JHEP* **04** (2019) 015 [arXiv:1811.03052] [ɪɴSPIRE].

[184] CMS collaboration, *Search for Excited Leptons in Proton-Proton Collisions at $\sqrt{s} = 8$ TeV*, *JHEP* **03** (2016) 125 [arXiv:1511.01407] [ɪɴSPIRE].